Rab10 regulates the sorting of internalised TrkB for retrograde axonal transport

Oscar M. Lazo[1,2] * and Giampietro Schiavo[1,2] *
[1] Department of Neuromuscular Diseases, UCL Queen Square Institute of Neurology, University College London, London WC1N 3BG, UK
[2] UK Dementia Research Institute at UCL, London WC1E 6BT, UK

* To whom correspondence should be addressed: Oscar Marcelo Lazo (oscar.lazo@ucl.ac.uk); Giampietro Schiavo (giampietro.schiavo@ucl.ac.uk)

Word count main text: 4,283
Word count abstract: 166
Figures: 8
References: 74
Supplementary items: 6 (1 Table, 2 Figures, 3 Videos)
Key words: Brain-derived neurotrophic factor, KIF13B, neurotrophin, signalling endosome, small GTPases

Abstract

Neurons process real-time information from axon terminals to coordinate gene expression, growth and plasticity. Input from distal axons is encoded as a stream of endocytic organelles, termed signalling endosomes, targeted to the soma. Formation of these organelles depends on target-derived molecules, such as brain-derived neurotrophic factor (BDNF), which is recognised by TrkB receptors on the plasma membrane, endocytosed and transported to the cell body along the microtubules network. Notwithstanding its neuropathological importance, the mechanism controlling the sorting of TrkB to signalling endosomes is currently unknown. In this work, we uncover the small GTPase Rab10 as critical for TrkB sorting and propagation of BDNF signalling from axon terminals to the soma. Our data demonstrate that Rab10 defines a novel class of axonal organelles, rapidly mobilised towards the axon terminal upon BDNF stimulation, enabling the axon to fine-tune retrograde signalling depending on BDNF availability at the synapse. These results help clarifying the neuroprotective phenotype recently associated to Rab10 polymorphisms and provide a new therapeutic target to halt neurodegeneration.

Introduction

Communication between cells depends on their ability to respond as integrated units to spatial and temporal signalling patterns. The complex morphology of neurons provides an unrivalled model to study how sorting and trafficking of signalling complexes coordinate local signalling at axon terminals and the propagation of

messages to the cell body. A clear example is provided by neurotrophic factors secreted by target tissues and sensed by axon terminals, where, among other functions, they regulate local cytoskeletal dynamics to promote or cease axon elongation, induce branching, as well as maturation and synaptic plasticity [1-3]. At the same time, a population of activated receptors are internalised and targeted to the retrograde axonal transport pathway within signalling endosomes [4,5], which propagate neurotrophic signalling towards the cell body, regulating gene expression, dendritic branching, and the equilibrium between survival and apoptosis [6-9]. How local and central responses are coordinated across the massive distance from axon terminals to the soma is a crucial and still unanswered question for neuronal cell biology.

Brain-derived neurotrophic factor (BDNF), a member of the neurotrophin family, is widely expressed in the central nervous system, together with its receptor tropomyosin-related kinase B (TrkB). By activating diverse signalling cascades, comprising the phosphoinositide 3-kinase (PI3K)-Akt pathway, mitogen-activated protein kinases (MAPKs) and phospholipase C-gamma (PLCγ), BDNF and TrkB play a critical role in the formation, maintenance and plasticity of neuronal circuits [10,11]. Binding of BDNF at synaptic sites leads to endocytosis of TrkB and entry of the activated ligand-receptor complexes in early endosomes [12]. Whilst part of internalised TrkB recycle back to the plasma membrane, a pool of receptors is sorted to signalling endosomes and engage with the cytoplasmic dynein motor complex, which mediates the transport of these organelles to the soma [1,9,13]. Independent lines of evidence indicate that this compartment is generated from early endosomes that then mature into a more specialised organelle escaping acidification and lysosomal degradation [5]. Sorting of TrkB receptors from early to signalling endosomes constitutes the critical regulatory node controlling the intensity of the retrogradely-propagated signal; however, to date no clear mechanism controlling this sorting process has been demonstrated.

The Rab family of monomeric GTPases plays a central role regulating post-endocytic trafficking of TrkB. Whilst early endosome formation is regulated by Rab5, maturation and processive transport of signalling endosomes in different neuronal models are controlled by Rab7 [12,14-16]. However, it is currently unclear whether or not Rab7 is the only member of the Rab family necessary for the latter process. Because axonal retrograde signalling endosomes appear to be a diverse group of organelles [5], we hypothesised that other members of the Rab family also contribute to the segregation of TrkB and its sorting to retrograde axonal carriers.

In this work, we specifically focused on Rab10, since it has been shown that Rab10-positive organelles are transported both anterogradely and retrogradely along axons in hippocampal neurons [17]. Previous work from

71 our laboratory using an affinity purification approach to isolate neurotrophin signalling endosomes from
72 mouse embryonic stem cell-derived motor neurons found that Rab10 was significantly enriched in this axonal
73 compartment, which is also characterised by the presence of Rab5 and Rab7 [18]. By manipulating Rab10
74 expression and activity in hippocampal neurons, as well as analysing the axonal dynamics of Rab10 organelles,
75 we have explored its ability to regulate the sorting of TrkB to the retrograde axonal transport pathway and
76 respond to increasing concentrations of BDNF, adjusting retrograde signalling on demand.
77

78 **Results**

79

80 *Decreasing the expression of Rab10 in neurons*

81 To manipulate Rab10 expression levels in hippocampal neurons, we used a lentiviral system encoding a
82 doxycycline-inducible short hairpin RNA (shRNA). We monitored the effects of this virus on cell viability and
83 expression levels of Rab10 and TrkB at different time points after doxycycline treatment. We observed that
84 48 hours of treatment consistently halved the number of cells per field compared to control group, whereas
85 incubation for 24 hours did not affect neuronal density (Figure 1a-b). Rab10 immunoreactivity appeared
86 significantly decreased at both 24 and 48 hours after addition of doxycycline, compared to control lentivirus
87 (Figure 1a and c). Finally, we monitored expression levels of TrkB receptors, to confirm that this system will
88 allow the study of the trafficking of the endogenous receptor upon Rab10 knockdown. We observed
89 comparable levels of TrkB even at 48 hours of treatment with shRNA Rab10 (Figure 1d).
90

91 *Rab10 is required for retrograde TrkB trafficking and signalling*

92 To study axonal TrkB dynamics, we cultured hippocampal neurons in microfluidic chambers, which allow the
93 cellular and fluidic compartmentalisation of axon terminals. After 7 days in vitro, neurons plated in one of the
94 compartments (designated as 'somatic') displayed axons reaching the axonal compartment (Figure 2a).
95 Maintaining a higher volume of media in the somatic compartment allows a micro-flow along the grooves,
96 keeping any substance added to the axonal compartment confined to this area. Using this experimental set
97 up, we incubated axon terminals with an antibody against the extracellular domain of TrkB and induced its
98 endocytosis by adding 20 ng/mL BDNF. After 2.5 hours, we were able to detect axonal TrkB in the cell body of
99 neurons stimulated with BDNF, but not in neurons depleted of BDNF by addition of an anti-BDNF blocking
100 antibody (Figure 2b), confirming the reliability of our retrograde accumulation assay.
101
102

Figure 1. Doxycycline-inducible knockdown of Rab10 in hippocampal neurons

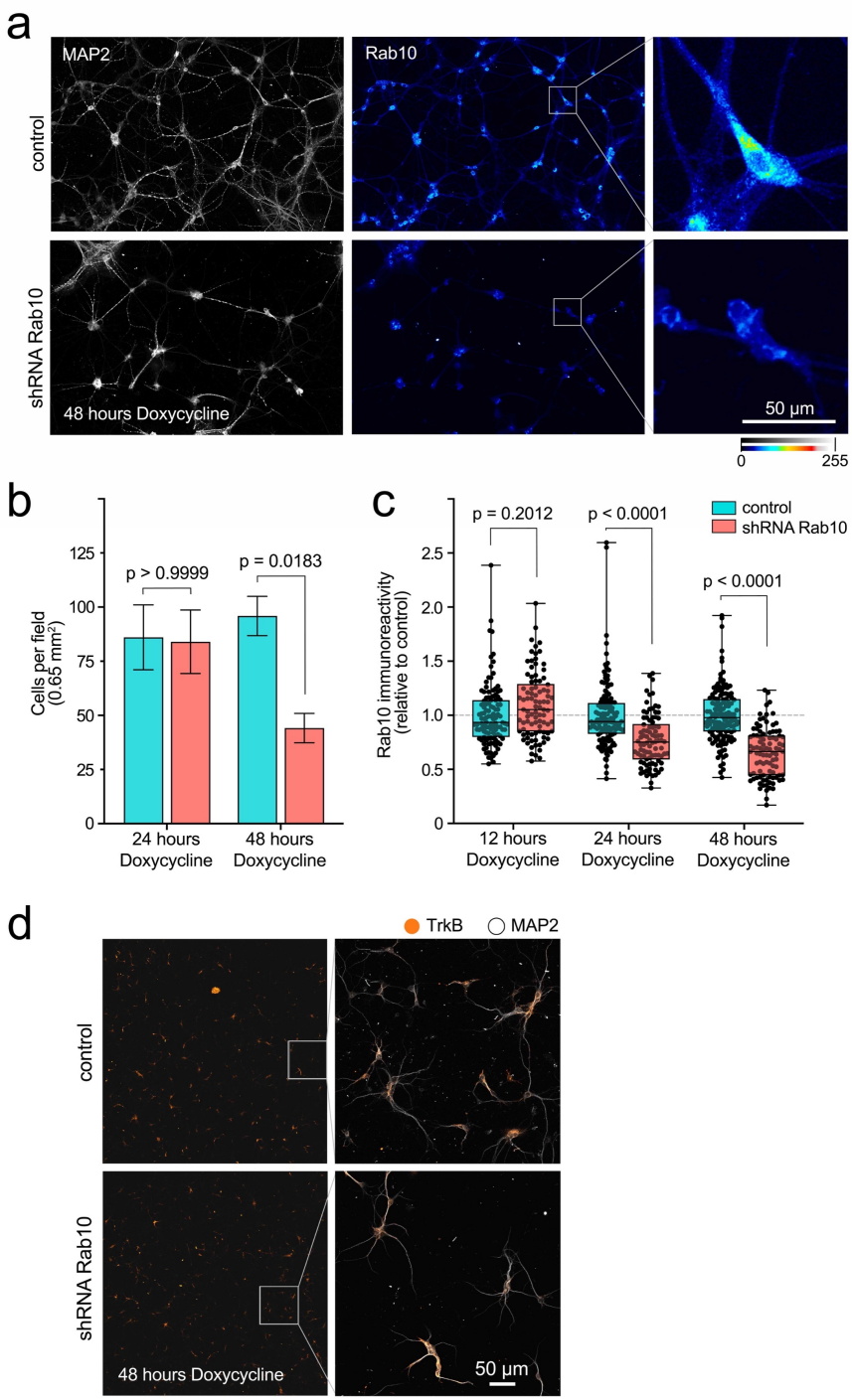

(a) Representative fields of a primary mass culture of hippocampal neurons transduced with shRNA Rab10 versus control and treated with doxycycline for 48 h, and immunolabelled for MAP2 (grey) and Rab10 (colour scale 0-255). Bar scale = 50 µm. **(b)** Cell density was quantified in 18 fields per treatment across 3 independent experiments, showing a significant decrease after 48 hours. Two-way ANOVA, F(1,68), p value for knockdown = 0.0270, p value for time = 0.0406, p value for interaction = 0.2114 (non-significant). The p values for Bonferroni multiple comparison tests, t(68), are indicated in the plot. **(c)** In the same experiments, immuno-reactivity for Rab10 was quantified per cell at 12, 24 and 48 h with doxycycline and analysed by using two-way ANOVA (p value for knockdown, time and interaction < 0.0001); p values for Bonferroni multiple comparison tests, t(68), are indicated in the plot and show significant effect of the shRNA at 24 and 48 h. **(d)** Representative low magnification fields showing no difference on immunoreactivity for TrkB in hippocampal neurons treated with shRNA Rab10 versus control after 48 hours with doxycycline. The right panel show zoomed boxes with TrkB (orange) and MAP2 (grey)

Neurons transduced with the shRNA Rab10 and treated with doxycycline for 18-22 hours showed lower levels of endogenous Rab10 (Figure 2c, grey) and significantly reduced retrograde accumulation of TrkB when compared with neurons expressing control lentivirus (Figure 2c-d). Since expression of Rab10 is variable among neurons, we tested the correlation between the levels of endogenous Rab10 with the retrograde accumulation of TrkB (Figure 2e). We found that, even though there was overlap, control and knocked down neurons clustered as expected.

Figure 2. Rab10 is required for retrograde TrkB trafficking and signalling.

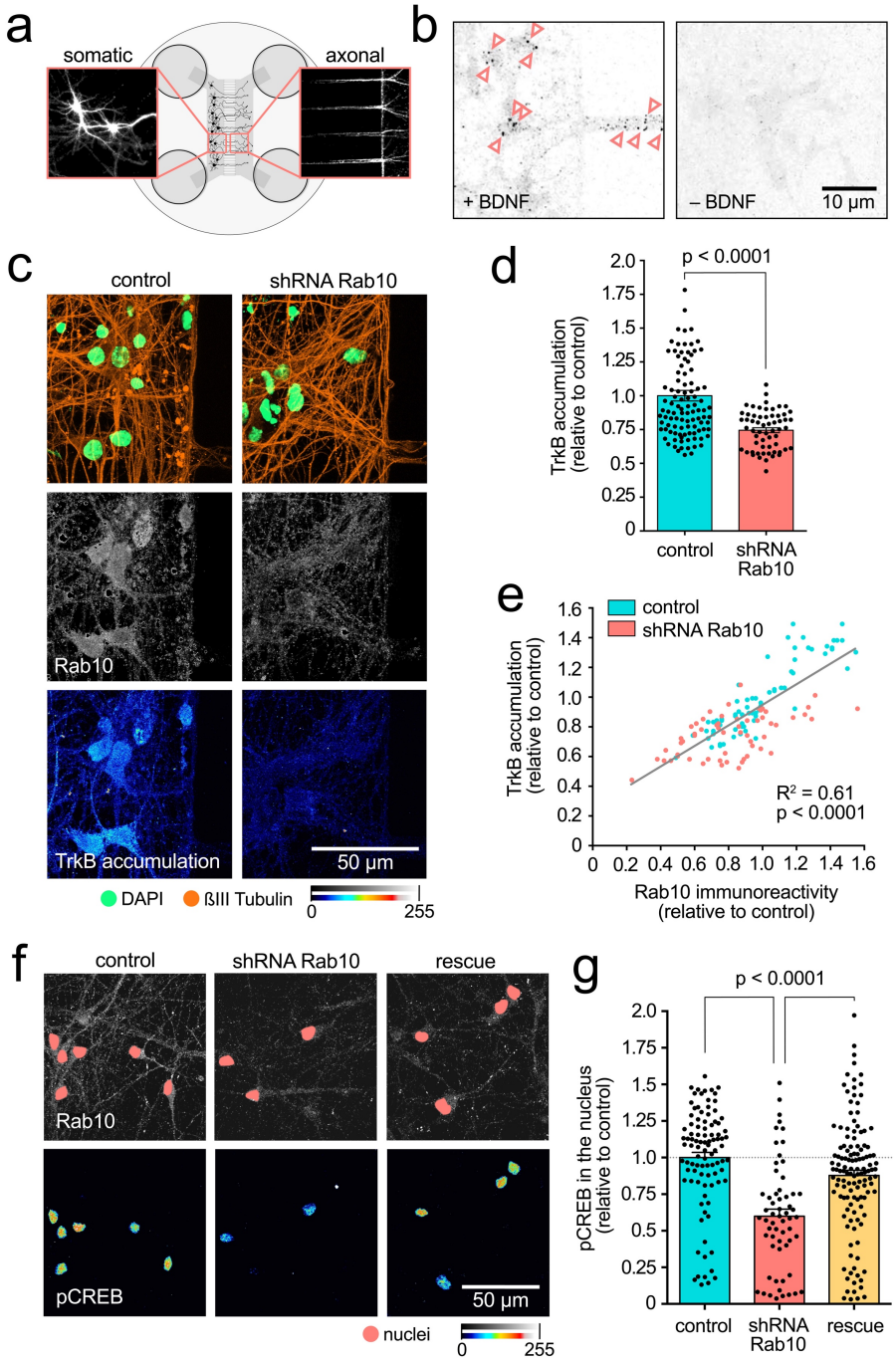

(a) Schematic of two-compartment microfluidic chambers highlighting compartimentalisation of somata (left) and axon terminals (right). Micro-flow from somatic to axonal compartments provides fluidic isolation of the somatic compartment to probes added to the other chamber. **(b)** Representative images from the cell bodies of neurons incubated for 2.5 hours with anti-TrkB in the axonal compartment, with (+) or without (-) BDNF. Pink arrowheads indicate examples of retrogradely transported TrkB-positive organelles. Scale bar: 10 µm. **(c)** Neurons treated with the shRNA targeting Rab10 were compared to control transduced neurons. Immunofluorescence revealed similar neuronal density (see ßIII-tubulin in orange and nuclear staining in green, top panel), but a decrease in both, expression of Rab10 (gray, middle panel) and retrograde accumulation of TrkB after 2.5 hours (colour intensity scale, bottom panel). Scale bar: 50 µm **(d)** Quantification of retrograde TrkB accumulation in three independent experiments show statistically significant differences (unpaired t-Student test, t(140), $p < 0.0001$). **(e)** Correlation between expression level of Rab10 and retrograde TrkB accumulation in control and Rab10-knockdown neurons show a significant linear correlation (Goodness of fit $R^2 = 0.61$; Pearson r, XY pairs= 131, $p < 0.0001$). **(f)** Axonal stimulation with BDNF for 2.5 hours leads to robust appearance of phosphorylated CREB in the nucleus of control neurons (left panel). This response was impaired in neurons depleted of Rab10 (middle panel), and rescued by the co-expression of a shRNA-resistant mutant Rab10 (right panel). Immunofluorescence for Rab10 is shown in grey, with the nuclei indicated with a pink mask, and nuclear phosphorylated CREB is shown in a colour intensity scale. Scale bar: 50 µm. **(g)** Quantification from three independent experiments showing the statistically significant effect of manipulating Rab10 expression on the levels of phosphorylated CREB in the nucleus (one-way ANOVA, F(2,280), $p < 0.0001$; p values for the Bonferroni multiple comparison tests, t(280), are indicated in the plot).

205 Moreover, when we take both populations together, we found a significant correlation between Rab10
206 expression and TrkB accumulation, strongly suggesting that Rab10 plays a role in retrograde axonal transport
207 of internalised TrkB (Figure 2e).
208
209 To confirm the functional consequences of this decrease on the retrograde transport of TrkB, we treated
210 neurons in the axonal compartment with BDNF and analysed the levels of phosphorylated cAMP response
211 element binding protein (pCREB) in the nucleus. pCREB is a well-established proxy for neurotrophic signalling
212 in neurons and has been shown to be critical for global neuronal responses to neurotrophins, such as BDNF-
213 induced dendritic branching [19]. Neurons treated with a shRNA directed against Rab10 showed a significant
214 decrease in nuclear pCREB (Figure 2f-g), which was completely rescued by treatment of Rab10 knockdown
215 cells with a lentivirus encoding shRNA-resistant Rab10, further confirming the specificity of this effect.
216
217 *Rab10 associates transiently to TrkB-containing retrograde carriers*
218 Given its critical role regulating retrograde accumulation of TrkB, we investigated whether Rab10 was present
219 in retrograde signalling endosomes. As stated before, signalling endosomes are likely to be a heterogeneous
220 pool of functionally-related organelles with diverse molecular compositions [5]. Most of these axonal carriers
221 are positive for Rab7 [12], which enables the recruitment of the dynein motor complex and their processive
222 retrograde transport along microtubules [9,13]. Endogenous Rab10 (orange) and Rab7 (green) were detected
223 with specific antibodies and imaged by confocal microscopy (Figure 3a). Co-localisation was evaluated using
224 Manders index and significance determined using confined-displacement algorithm (CDA) [20]. Rab10 and Rab7
225 were found to exhibit very low co-localisation levels (Figure 3a, yellow arrowheads), both in neurons
226 stimulated with BDNF (20 ng/mL for 30 min), as well as in neurons depleted of BDNF by treatment with a
227 blocking antibody (Figure 3b). Super-resolution radial fluctuations (SRRF) microscopy was used to examine the
228 distribution of Rab10, Rab7 and Rab5 along the axon of neurons stimulated with BDNF as described above
229 (Figure 3c). We found that Rab10 and Rab7 consistently showed a very low degree of overlap (see yellow
230 regions in Figure 3c and super position of intensity peaks in 3d). On the other hand, this super-resolution
231 approach revealed a population of organelles where Rab10 and Rab5 partially co-localise (pink regions, Figure
232 3c-d), suggesting that Rab5-positive retrograde carriers [21], or stationary early endosomes, could contain
233 Rab10. To identify retrograde signalling endosomes containing TrkB, we took advantage of the property of the
234 non-toxic carboxy-terminal domain of the heavy chain of tetanus neurotoxin (H_CT) of being transported almost
235 exclusively in retrograde axonal organelles in neurons [12]. We co-internalised H_CT-AlexaFluor 647 and mouse
236 anti-Flag antibodies in neurons transfected with a TrkB-Flag construct, and stimulated them with BDNF.

Figure 3. Internalised TrkB transiently co-localises with Rab10 in axons.

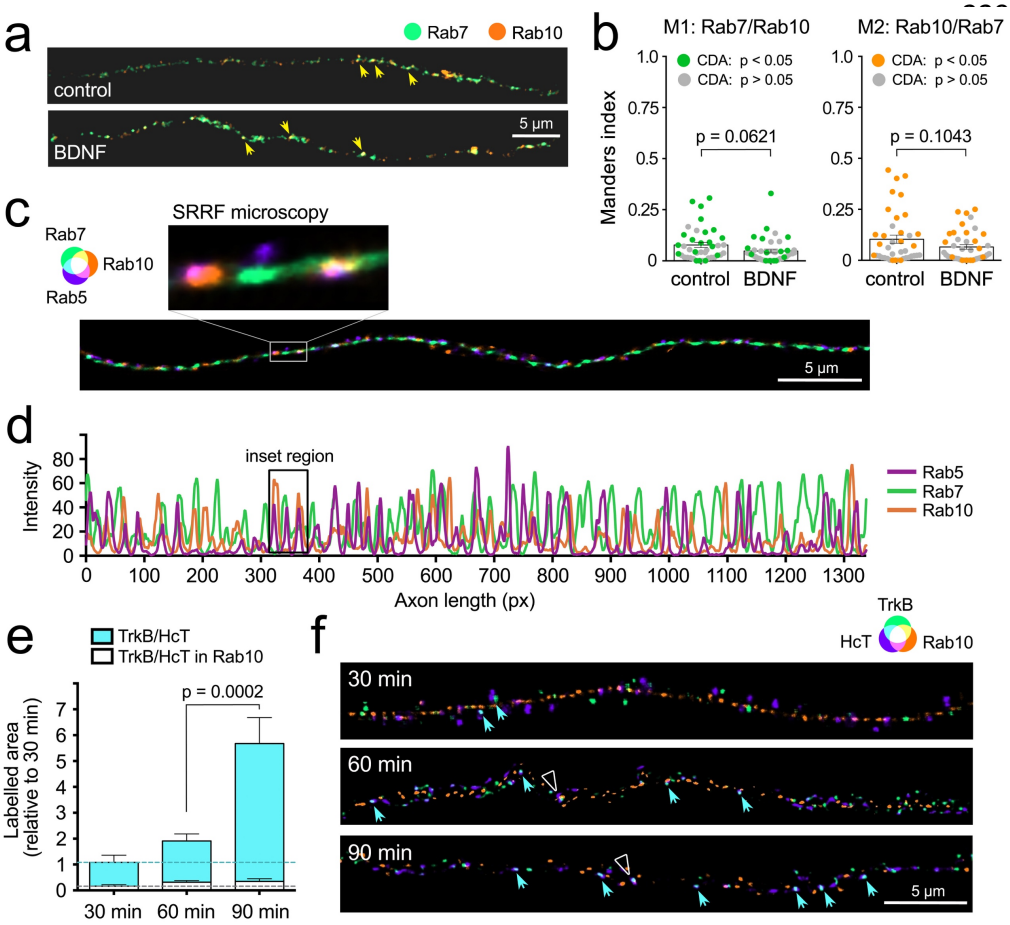

(a) The distribution of endogenous Rab10 (orange) and Rab7 (green) was monitored using confocal microscopy in axons with or without BDNF treatment for 30 min. Points where both markers overlap are indicated with yellow arrowheads. Scale bar = 5 µm. **(b)** Co-localisation was analysed using confined-displacement algorithm (CDA), and Manders coefficients were compared for control versus BDNF-treated axons (Welch's corrected Unpaired t-Student; M1: t(72.32), p value = 0.0621; M2: t(62.33), p value = 0.1043). Data points showing significant co-localisation compared to random distribution are marked with coloured dots. No significant differences were found between starved and BDNF-stimulated neurons. **(c)** Representative SRRF microscopy of an axon stained for endogenous Rab5 (purple), Rab7 (green) and Rab10 (orange). The inset at 6x higher magnification shows examples of partial co-localisation of Rab10 with Rab5 and Rab7. Scale bar = 5 µm. **(d)** Intensity along the same axonal segment shown in (c) was plotted to observe the correlation between the three markers. The region shown in the inset is indicated. Several examples of partial coincidence between Rab10 and Rab5 are observed. Overlap between Rab10 and Rab7 peaks is less frequent, confirming the data in (a) and (b). **(e)** Labelled H_CT and anti-TrkB were co-internalised in the presence of BDNF for 30, 60 and 90 min, and their level of overlap with endogenous Rab10 in axons was evaluated using confocal microscopy. Relative areas positive for H_CT and TrkB are shown in cyan (normalised to 30 min) and the fraction of the normalised area that was triple positive for H_CT, TrkB and Rab10 is plotted in white. Whereas the double TrkB/H_CT-positive area significantly increased by 90 min (one-way ANOVA, F(2,72), p value < 0.0001; Bonferroni multiple comparison test p value is shown in the plot), the triple TrkB/H_CT/Rab10 surface remained low and fairly constant at all time points (one-way ANOVA, F(2,72), p value = 0.2730; Bonferroni multiple comparisons test for 60 versus 90 min, t(72), p value > 0.9999). **(f)** Representative SRRF microscopy from the same three time points. Double positive puncta for TrkB (green) and H_CT (purple) is indicated with cyan arrowheads. Triple positive puncta of TrkB/H_CT (cyan) and Rab10 (orange) are indicated with white empty triangles. Scale bar = 5 µm.

Axonal double-positive TrkB/H_CT puncta were considered signalling endosomes moving in the retrograde direction, and we analysed the proportion of these organelles colocalising with Rab10. Figure 3e represents the relative area of TrkB/H_CT and the triple positive area of TrkB/H_CT/Rab10 across three different time points (30, 60 and 90 minutes) post-endocytosis. As expected, the amount of TrkB in retrograde carriers increases

290 with time (cyan). However, the proportion of TrkB present in Rab10 organelles is very low and remains
291 constant across the duration of the experiment (white). These results suggest that TrkB localises transiently
292 on Rab10-positive organelles *en route* to its delivery to axonal retrograde carriers. This observation is
293 supported by super-resolution images (Figure 3f), showing an increase of TrkB/H_CT double-positive puncta
294 (cyan arrowheads), but very few TrkB/H_CT/Rab10 triple-positive puncta (white empty triangles) at 60 and 90
295 minutes.
296
297 *Overexpressed Rab10 is co-transported with retrograde TrkB*
298 The data presented so far support a model in which Rab10 is critical for retrograde transport of TrkB, but does
299 not specifically define a stable population of retrograde carriers. Rather, the evidence shown in Figure 3e-f
300 suggests that TrkB is transiently associated to Rab10-positive organelles, opening the possibility that Rab10
301 participates in the sorting of internalised receptors to retrogradely transported signalling endosomes. To
302 directly monitor this process, we overexpressed Rab10-EGFP in primary hippocampal neurons. Since it is well
303 documented that overexpression of Rab GTPases promotes their activity due to their increased association to
304 membranes [22], we expected that an increase in the abundance and/or activity of Rab10 stabilises its
305 association to TrkB retrograde carriers, allowing its visualisation by time-lapse microscopy. Neurons were co-
306 transfected with Rab10-EGFP and TrkB-Flag and, after 1 hour of starvation in non-supplemented Neurobasal
307 medium, we internalised AlexaFluor647-labelled anti-Flag antibodies in the presence of BDNF for 45 min
308 (Figure 4a). Time-lapse confocal imaging of axon segments was performed at least 200 µm from the cell body.
309 Sequential frames of a representative movie are shown in Figure 4b, where the retrograde co-transport of
310 TrkB and Rab10-EGFP is indicated with yellow arrowheads. Kymographs (Figure 4c) were generated for Rab10-
311 EGFP (orange) and TrkB-Flag (green). Tracks are shown in the bottom panel, with examples of co-transport
312 indicated by yellow lines. Quantification of five independent experiments confirmed that approximately 60%
313 of retrograde TrkB carriers are positive for Rab10 under these experimental conditions (Figure 4d).
314 Interestingly, no anterograde TrkB/Rab10 double-positives compartments were observed, suggesting that
315 TrkB is present in organelles with a strong retrograde bias.
316
317 To extend this analysis to the other physiological BDNF receptors, the internalisation of endogenous p75
318 neurotrophin receptor ($p75^{NTR}$) was monitored in neurons expressing Rab10-EGFP. After depletion of trophic
319 factors, $p75^{NTR}$ uptake was visualised by incubating neurons for 45 min with an AlexaFluor 647-labelled
320 antibody against the extracellular domain of $p75^{NTR}$, in the presence of BDNF (Figure 4e).
321

Figure 4. Over-expressed Rab10 is co-transported with TrkB and p75 receptors in the axon.

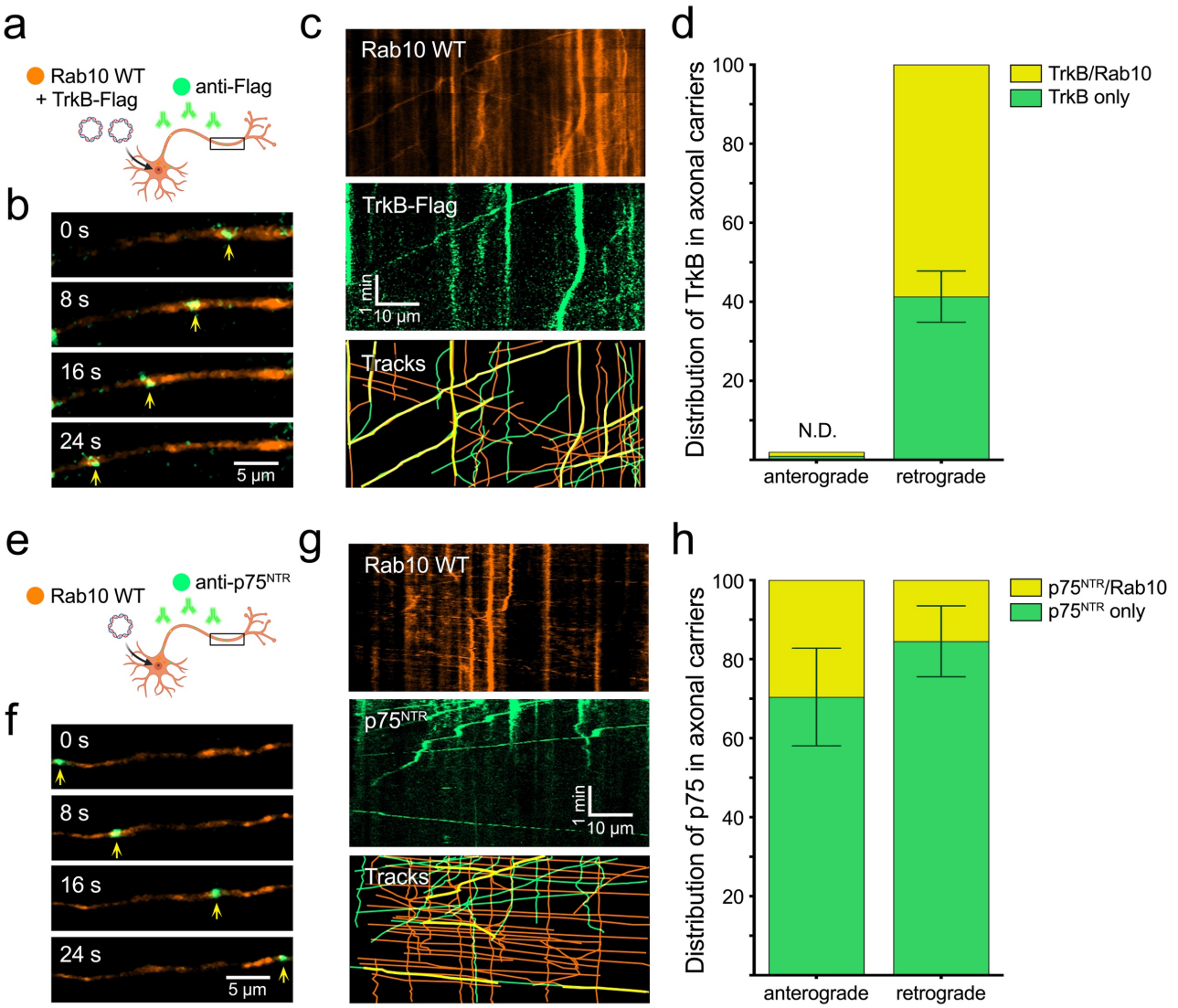

(a) Hippocampal neurons in mass culture were co-transfected with Rab10-EGFP and TrkB-Flag plasmids. Fluorescently-labelled anti-Flag antibodies were internalised in the presence of BDNF and their axonal dynamics monitored by time-lapse microscopy. **(b)** Representative images of the axon of a double transfected neuron, where a double-positive organelle for Rab10-EGFP (orange) and anti-Flag (green) is indicated with yellow arrowheads. Scale bar = 5 µm. **(c)** Representative kymograph of the axon of a double transfected neuron during 5 minutes of imaging showing Rab10 and TrkB-Flag channels. Double-positive tracks (in yellow) show transport predominantly in the retrograde direction (right to left). Scale bar = 10 µm. **(d)** Quantification of five experiments showing the proportion of TrkB-containing mobile organelles that were positive for Rab10. No anterograde TrkB organelles were found; therefore, presence of Rab10 could not be determined (N.D.). **(e)** An equivalent experiment was performed by transfecting Rab10-EGFP and visualising it together with endocytosed fluorescently-labelled anti-$p75^{NTR}$ antibodies. **(f)** Representative frames from a time-lapse movie displaying a double-positive organelle for Rab10 (orange) and $p75^{NTR}$ (green) moving anterogradely. Scale bar = 5 µm. **(g)** Representative kymograph showing Rab10 and $p75^{NTR}$ channels. Double-positive tracks (in yellow) show transport in both anterograde (left to right) and retrograde directions. Scale bar = 10 µm. **(h)** Quantification of five experiments displaying the proportion of $p75^{NTR}$ mobile organelles positive for Rab10 moving in the anterograde and retrograde direction.

Live-cell imaging of axon segments was done under conditions identical to those used for TrkB. Representative frames and kymographs of Rab10-EGFP (orange) and internalised $p75^{NTR}$ (green) are shown in Figure 4f-g. Interestingly, $p75^{NTR}$ receptor can be found in both retrograde and anterograde Rab10 organelles. On average, 29.6% of anterograde and 15.5% of retrograde $p75^{NTR}$ carriers were found positive for Rab10 across five independent experiments (Figure 4h).

BDNF promotes anterograde trafficking of Rab10-positive compartments

In agreement with the bidirectional transport observed for $p75^{NTR}$-containing organelles (Figure 4h), previous work suggested that Rab10-positive compartments travel along the axon in both directions [17]. In light of these results, we hypothesised that the dynamics of Rab10 organelles may respond to BDNF signalling to direct the sorting of TrkB to retrograde carriers. We therefore examined the axonal transport of Rab10-positive organelles in hippocampal neurons under two opposite conditions: depletion of BDNF using an anti-BDNF blocking antibody, followed by stimulation with 50 ng/mL BDNF (Supplementary Video 1).

Figure 5. BDNF regulates the directionality of Rab10 organelles.

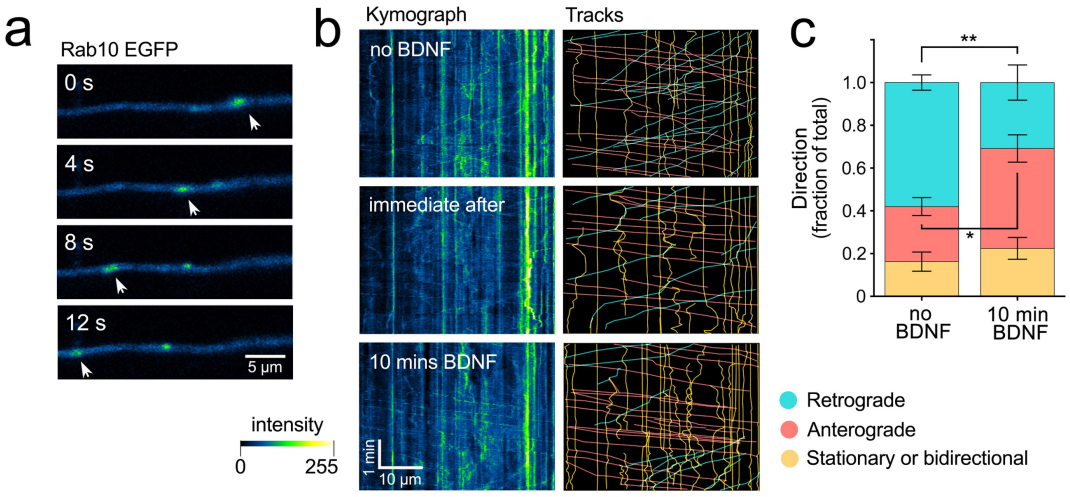

Hippocampal neurons in mass culture were transfected with Rab10-EGFP and depleted of BDNF for 60 minutes. **(a)** Representative axon of a live neuron showing retrograde (right to left) transport of a Rab10-positive organelle (white arrowheads) in the absence of BDNF. Scale bar = 5 µm. **(b)** In the panels on the left, representative kymographs (colour-coded as in a) are presented from the same axon upon BDNF depletion (top), immediately after the addition of 50 ng/mL of BDNF (middle) and 10 minutes thereafter (bottom). In the panels on the right, tracks have been traced and categorised as retrograde (cyan), anterograde (pink) or stationary/bidirectional (yellow). Scale bar = 10 µm. **(c)** The frequencies of tracks from each of the three categories have been quantified and plotted, comparing no BDNF and 10 minutes post-addition of 50 ng/mL BDNF. N= 14 axonal segments from 10 independent experiments. Unpaired t-Student, t(14), showed a significant increase in anterograde carriers (p value = 0.0150, *) at the expense of retrograde carriers (p value = 0.003, **). Stationary and bidirectional carriers did not show any significant change (p value = 0.4278). See Supplementary Video 1.

385 Figure 5a shows representative frames of a Rab10-EGFP organelle moving in the retrograde direction along
386 the axon (white arrows) in the absence of BDNF. Five minutes segments of time-lapse microscopy have been
387 used to generate kymographs (Figure 5b) at different time points of BDNF stimulation: before BDNF (top),
388 immediately after BDNF addition (centre) and after 10 min of BDNF incubation (bottom). Traces have been
389 colour-coded as retrograde (cyan), anterograde (pink) or stationary/bidirectional (yellow) to reveal changes in
390 the direction bias of Rab10 organelles in the same axon, before and after the addition of BDNF. Quantification
391 of five independent experiments shows that BDNF-depleted axons exhibit a bias towards retrograde Rab10
392 transport, which significantly switches to anterograde after 10 min of stimulation with BDNF.
393
394 These surprising results reveal a novel mechanism ensuring a tight balance between retrograde and
395 anterograde transport of Rab10 organelles, which is fine-tuned by BDNF. This result predicts that any local
396 increase in BDNF release from post-synaptic compartments will increase the abundance of Rab10 organelles
397 in the immediate vicinity of the source of BDNF.
398
399 *BDNF increases the recruitment of KIF13B to Rab10 organelles in the axon*
400 The uniform polarity of the microtubules in the axon of mature neurons implies that the directionality of
401 axonal carriers largely depends on their association to anterograde or retrograde motor proteins [23,24]. To
402 provide further mechanistic insights into the directional switch of Rab10 axonal organelles upon BDNF
403 stimulation, we analysed the distribution of two anterograde microtubule-associated motor proteins
404 predominantly found in central neuron axons, KIF5B and KIF13B [25]. Figures 6a and d show representative high-
405 resolution confocal microscopy images of axons where endogenous Rab10 (green) and either KIF13B or KIF5B
406 (orange) have been co-labelled. Neurons were either starved in the presence of a blocking anti-BDNF antibody
407 (control) or treated for 30 min with 50 ng/mL BDNF (BDNF). Insets displaying two different views of 3-
408 dimensional reconstructions of axonal segments show Rab10 organelles positive for KIF13B (Figure 6a) or
409 KIF5B (Figure 6d), in the absence and presence of BDNF. Interestingly, the axonal pool of KIF13B appears to
410 decrease after stimulation with BDNF, whereas that of KIF5B increases under the same experimental
411 conditions, suggesting that the total axonal content of these kinesins is differentially regulated by BDNF
412 signalling.
413
414
415
416

Figure 6. BDNF increases recruitment of KIF13B to Rab10 domains.

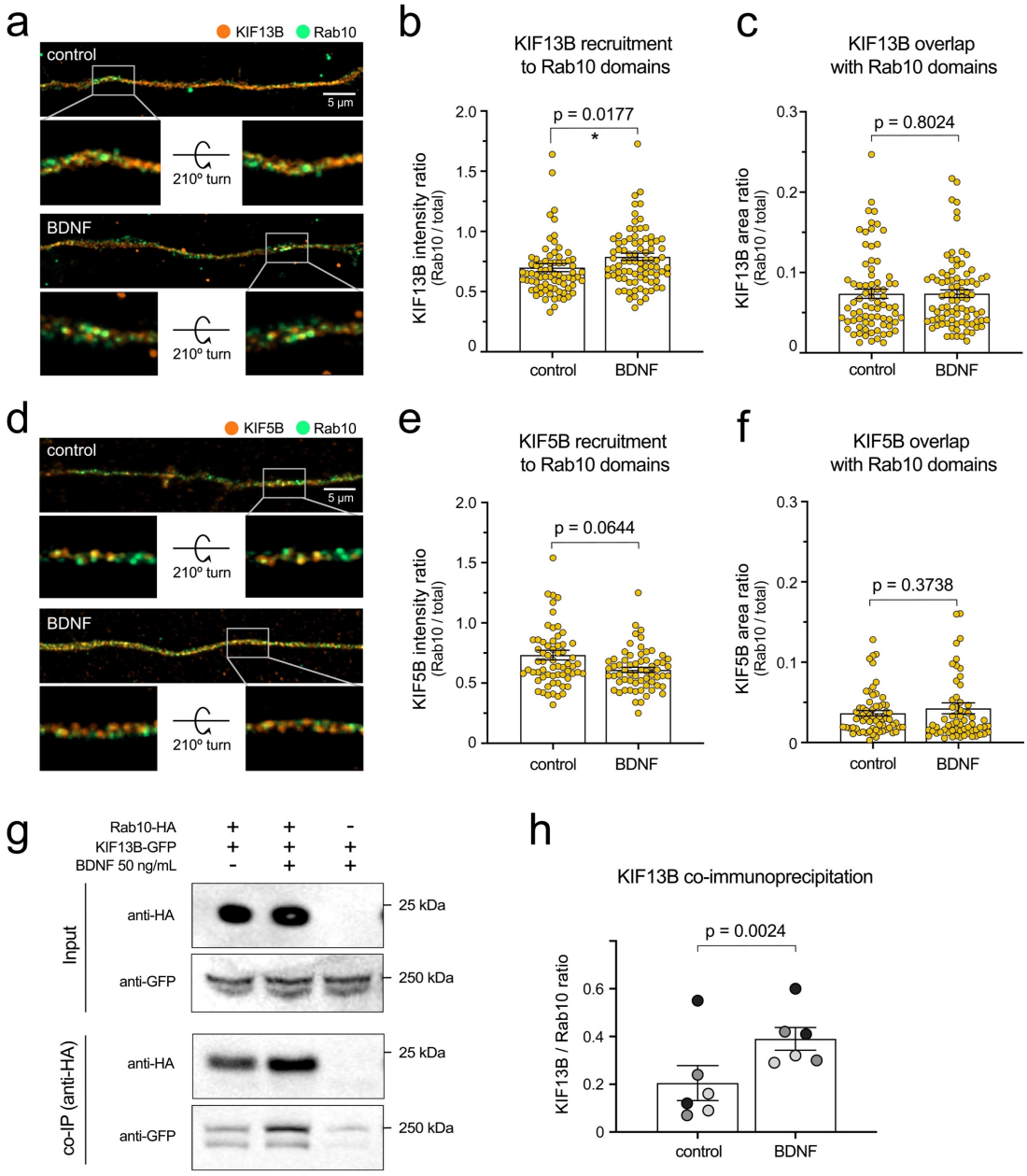

(a) The co-distribution of endogenous KIF13B (orange) and Rab10 (green) was monitored using high-resolution Airyscan confocal microscopy in axons of neurons with or without BDNF for 30 minutes. Top images correspond to maximum projection of z-stacks, scale bar = 5 µm. A 3D reconstruction of the inset area (grey frame) is shown for each top image on its original position and after turning the image 210° around the x axis. **(b)** KIF13B intensity was measured in the entire axon segment and in Rab10 positive areas, and the intensity ratio was plotted and analysed showing a significant enrichment of KIF13B in Rab10 areas upon 30 min of BDNF stimulation (Kolmogorov-Smirnoff nonparametric t test, t(79.5), p value = 0.0177). **(c)** Ratio between KIF13B-positive area that overlaps with Rab10 from total KIF13B area was plotted, finding no difference between neurons starved or incubated with BDNF 30 min (Kolmogorov-Smirnoff nonparametric t test, t(79.5), p value = 0.8024). **(d)** Co-distribution of KIF5B (orange) and Rab10 (green) was also analysed and displayed as in (a). Scale bar = 5 µm. Insets show 3D reconstructions on their original and rotated position. **(e)** Quantification of intensity ratio of KIF5B in Rab10 domains versus total KIF5B in the axon shows no significant difference between starved and BDNF-treated neurons (Kolmogorov-Smirnoff nonparametric t test, t(62.5), p value = 0.0644). **(f)** Proportion of the KIF5B-positive area that overlaps with Rab10 is lower than KIF13B and is not altered by BDNF stimulation (Kolmogorov-Smirnoff nonparametric t test, t(62.5), p value = 0.3738). **(g)** The interaction of Rab10-HA and KIF13B-GFP from N2A cells is modulated by BDNF. Top panel, representative western blot showing the presence of both proteins in the lysate (Input). Bottom panel, western blot of co-immunoprecipitated samples from the same experiment using an antibody against the HA tag. **(h)** Quantification of the ratio between normalised KIF13B and Rab10 in 3 independent experiments. Western blots have been done in duplicate and the corresponding paired experiments are indicated by data points of the same shade of grey. Groups were compared using paired t-student test, t(6), p value = 0.0024.

475 Quantification of the intensity of KIF13B in Rab10-positive areas (Figure 6b) reveals a statistically significant
476 12.7% increase in the amount of the motor recruited to Rab10-positive organelles. On the other hand, Figure
477 6c shows that the ratio between the Rab10-positive and total KIF13B positive area in the axon remained
478 unchanged (7.3% of the area), suggesting that the proportion of double KIF13B/Rab10 organelles remains
479 constant. In contrast, when we performed the same analysis for KIF5B, we found that, despite its global
480 increase in the axon upon BDNF stimulation, there is no significant change in the intensity ratio in Rab10-
481 positive domains, with a trend towards decrease (Figure 6e). Consistently, Figure 6f shows that the proportion
482 of KIF5B axonal organelles that overlap with Rab10 is lower than KIF13B (around 4% of the area) and remained
483 unchanged after BDNF stimulation.
484
485 Prompted by the results shown in Figure 6b, we investigated whether KIF13B and Rab10 interact in a BDNF-
486 dependent manner by expressing KIF13B-GFP and Rab10-HA in Neuro-2A (N2A) cells. This mouse
487 neuroblastoma cell line expresses TrkB and has been previously used in our laboratory to study trafficking and
488 signalling of neurotrophic receptors [26]. After 1 hour of starvation, transfected cells were treated or not with
489 BDNF 50 ng/mL and then we used anti-HA-conjugated magnetic beads to pull down Rab10-HA. Lysates, as well
490 as the co-immunoprecipitated samples eluted from the beads, were analysed by western blot. A
491 representative example is shown in Figure 6g, with the top panels showing the total amount of Rab10-HA and
492 KIF13B-GFP in the lysates (input). Co-immunoprecipitated Rab10-HA and KIF13B-GFP eluted from the beads
493 are displayed in the bottom panels (co-IP). Lysates from N2A cells only expressing KIF13B-GFP were used as
494 controls. Quantification of three independent experiments (Figure 6h) show an average twofold increase in
495 the KIF13B/Rab10 ratio when cells were stimulated with BDNF.
496
497 *Rab10 regulates the sorting of TrkB in early endosomes, with no effect on recycling*
498 After endocytosis, TrkB accumulates in early endosomes, from which it is sorted either to the recycling route
499 or to endosomal organelles with signalling capabilities [9,12]. Rab10, on the other hand, has been shown to
500 regulate trafficking across early endosomes, the formation of specialised tubular endosomes, the recycling of
501 cargoes back to the plasma membrane, as well as the targeting of plasmalemmal precursor vesicles (PPVs),
502 among other functions [17,27-30]. To understand the mechanism linking Rab10-positive organelles with the
503 retrograde axonal transport of TrkB in signalling endosomes, we designed experiments to discern between a
504 potential role of Rab10 on recycling of internalised TrkB back to the plasma membrane, and sorting of TrkB
505 out of early endosomes into retrograde transport carriers (Figure 7a).
506

507 **Figure 7. Rab10 regulates sorting of TrkB out of early endosomes.**

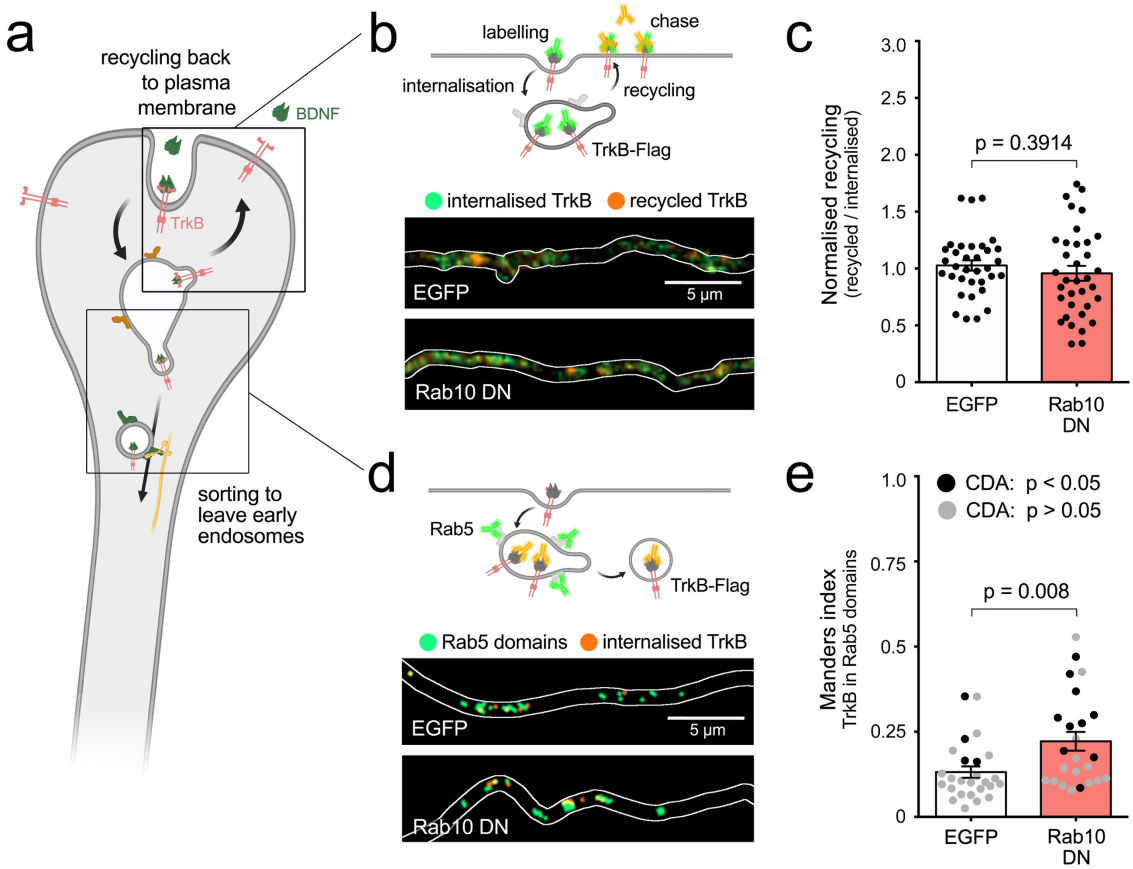

508
509 **(a)** Main hypotheses about the role of Rab10 regulating the sorting of TrkB to signalling endosomes include recycling back to the plasma
510 membrane or sorting of TrkB receptors out of early endosomes to retrograde carriers. **(b)** Top, diagram of the experiment showing
511 TrkB-Flag receptors on the axonal surface bound to anti-Flag antibodies (green). After internalisation, the remaining anti-Flag is
512 removed from the surface and the labelled receptor that recycled to the plasma membrane is chased with a secondary antibody
513 (orange). Bottom, representative examples of internalised TrkB (green) and recycled TrkB (orange) in axons from neurons transfected
514 with EGFP or a Rab10 DN mutant. **(c)** Normalised recycling shows no difference between EGFP and Rab10 DN transfected neurons.
515 Unpaired t-Student, t(60.40), p value = 0.3914. **(d)** Top, diagram of the internalisation of TrkB-flag labelled with anti-Flag antibodies
516 (orange) to Rab5-positive early endosomes (green). Bottom, representative thresholded microscopy images from the axon of neurons
517 transfected with EGFP or Rab10DN mutant. While the amount of orange puncta is similar in both conditions, yellow areas showing co-
518 localisation of internalised TrkB and Rab5 are increased upon Rab10 DN expression. **(e)** Quantification of co-localisation between
519 internalised TrkB-Flag and endogenous Rab5 is significantly higher in neurons expressing Rab10DN compared to EGFP. Unpaired t-
520 Student, t(38.22), p value = 0.008. Significant co-localisation according to CDA (p value < 0.05 compared to randomised signal) is shown
521 with black circles, while inconclusive co-localisation (p value > 0.05) is shown in grey. Scale bars = 5 µm.
522

523 To assess the contribution of Rab10 to the recycling of TrkB in the axon, hippocampal neurons were
524 transfected with EGFP or a dominant negative mutant of Rab10 (Rab10^{T23N}; referred as Rab10DN) and TrkB-
525 Flag. As illustrated in figure 7b, endocytosis of anti-Flag M1 antibodies was allowed for 30 minutes in the
526 presence of BDNF, and then the remaining antibody still bound to the neuronal surface was removed using
527 EDTA, which dissociates this antibody from the bound Flag peptide [31]. Recycling receptors were then chased
528 using AlexaFluor 647-conjugated secondary antibodies. After fixation, internalised TrkB-Flag was labelled with

529 AlexaFluor 555-conjugated secondary antibodies. Comparison between recycling ratio (recycled/internalised)
530 of EGFP- and Rab10DN-expressing neurons shows no significant differences (Figure 7c).
531
532 In contrast, if the sorting of TrkB to retrograde signalling carriers was regulated by Rab10, expression of
533 Rab10DN would result in the trapping a population of TrkB in early endosomes, driving an increase of co-
534 localisation between internalised TrkB and Rab5. Therefore, we incubated neurons transfected with TrkB-Flag
535 and either EGFP or Rab10DN, with anti-Flag antibodies for 30 min in the presence of BDNF, and then analysed
536 TrkB/Rab5 co-localisation using Manders index and CDA (Figure 7d-e). Rab10DN caused a statistically
537 significant increase of internalised TrkB in Rab5-positive domains from 13.2% ± 1.7 to 22.2% ± 2.8, and an
538 increase in the reliability of the co-localisation measurements (CDA $p < 0.05$) (Figure 7e). These results indicate
539 that the probability of finding axonal TrkB in Rab5-positive early endosomes increases in neurons expressing
540 Rab10DN, thus indicating that Rab10 modulates the sorting of activated TrkB receptors from axonal early
541 endosomes to retrograde transport organelles.
542

543 ## Discussion
544
545 Our results unravel a novel role for Rab10 in regulating the sorting of internalised TrkB receptors to the
546 retrograde axonal transport pathway. This function appears to be necessary not only for efficient trafficking
547 of TrkB from axons to soma, but also for the propagation of neurotrophic signalling from distal sites to the
548 nucleus, as shown by the decrease of BDNF-induced CREB activation upon Rab10 knockdown (Figure 2). CREB
549 is a transcription factor supporting neuronal survival and differentiation, which is activated by phosphorylation
550 downstream Akt and MAPK signalling [32]. Some of the better characterised early response genes to
551 neurotrophic factors (e.g., Egr1, Egr2, Arc and cFos) are transcriptional targets of CREB, which is also required
552 for BDNF-induced dendritic branching [19,33,34]. Therefore, CREB phosphorylation is one of the best proxies for
553 global responses to neurotrophic signalling. Long-distance activation of CREB has been reported from distal
554 axons and dendrites, and the endosomal trafficking of phosphorylated TrkB and signalling interactors has been
555 shown to play a crucial role in propagating neurotrophin signalling from the periphery to the nuclear pCREB
556 [8,35,36]. In our study we found that Rab10 expression was critical for maintenance and survival of differentiated
557 neurons, since its downregulation for 48 hours led to a significant decrease in neuronal density (Figure 1).
558 Similar effects have been reported upon overexpression of dominant-negative mutants of Rab5, the GTPase
559 mediating the formation of early endosomes, but not for Rab11, which controls the recycling of receptors to

560 the plasma membrane [37,38], suggesting that these distinct arms of the endosomal network differentially impact
561 on neuronal homeostasis.
562
563 Acting as a highly specialised network, Rab GTPases are master regulators of specific membrane trafficking
564 events in eukaryotic cells [36]. Rab10 is one of the few exceptions to this rule and during the last 30 years, it has
565 been associated to multiple trafficking pathways, including polarised exocytosis from early endosomes,
566 exocytosis in adipocytes and neurons, endoplasmic reticulum dynamics and the formation of tubular
567 endosomes, to cite but a few [39]. This multiplicity of functions is reflected by the diversity of its interactors and
568 effectors, emphasising the importance of the specific context in which Rab10 operates. Here we have
569 confirmed previous findings showing that Rab10-positives organelles are present in the axon of hippocampal
570 neurons and undergo bi-directional transport [17]. Importantly, in this work we have demonstrated that the
571 balance between anterograde and retrograde transport is regulated by BDNF, indicating the ability of Rab10
572 to specifically respond to extracellular cues in a signalling context. A similar function of Rab10 balancing
573 anterograde and retrograde transport has been shown to be required for correct dendritic patterning in
574 *Drosophila* [40].
575
576 We hypothesised that the differential recruitment of members of the kinesin superfamily of anterograde
577 motors could explain a rapid change in the directionality of Rab10 organelles. Given that many kinesins
578 distribute preferentially to distinct neuronal compartments [41], we focused on two kinesins that have been
579 found to be predominant in axons, KIF5B and KIF13B [25]. We found that KIF13B, but not KIF5B, increased its
580 relative abundance in axonal Rab10-positive domains (Figure 6a-f), which is in line with the recent evidence
581 indicating a direct interaction between Rab10 and KIF13A and B, via a Rab-binding domain (RBD-) homology
582 domain [29]. Moreover, when we used immunoprecipitation to investigate the interaction of KIF13B and Rab10,
583 we found that their binding significantly increases in the presence of BDNF (Figure 6g-h). Interestingly, KIF13B
584 and other members of the kinesin-3 family have been shown to yield super processive motion when acting as
585 dimers [42], helping to explain how even a relatively small increase in the recruitment of KIF13B onto axonal
586 Rab10-positive organelle can trigger a rapid change in their transport directionality.
587
588 Although the main focus of this work has been demonstrating a novel role of Rab10 in the retrograde
589 propagation of neurotrophic signalling, the recruitment of KIF13B onto Rab10-positive organelles is a crucial
590 finding to start disentangling the mechanisms that control the BDNF-dependent switch between retrograde
591 and anterograde transport. For example, the activity of Rab10 is known to be controlled by PI3K-Akt, a

592 canonical BDNF/TrkB signalling pathway. In adipocytes and muscle cells, Rab10 is known to regulate the
593 plasma membrane delivery of the glucose transporter GLUT4 in response to insulin, where activation of Akt
594 leads to phosphorylation of the Rab GAP Akt substrate of 160 kDa (AS160). Rab10 associated to GLUT4-
595 containing endosomes is kept inactive by AS160, until Akt signalling releases the brake and promotes fusion
596 with the plasma membrane [43]. However, two key observations suggest that directionality of Rab10 organelles
597 in the axon does not depend uniquely on Rab10 activity. First, both anterograde and retrograde organelles
598 have membrane-bound Rab10 (Figure 5), which is generally accepted to be its GTP-bound active form. Second,
599 we observed that the constitutively active $Rab10^{Q68L}$ mutant is transported predominantly in the retrograde
600 direction in neurons depleted of BDNF (see Supplementary Figure 1). Altogether, these findings indicate that
601 whilst the GTP-bound conformation of Rab10 is necessary to drive its binding to the membrane of axonal
602 organelles, this alone is not sufficient to determine the direction of transport.
603
604 The LRRK2-dependent phosphorylation of Rab10 in the highly conserved switch II region has been proposed
605 to affect its GTP/GDP cycle as well as its ability to bind effectors [44,45]. Moreover, this phosphorylation site has
606 been shown to regulate the interaction of Rab10 with JIP3 and JIP4 [46], which are adaptors for the plus-end-
607 directed microtubule-dependent motor kinesin-1 [47,48]. Interestingly, JIP3 has been shown to mediate the
608 anterograde transport of TrkB in neurons and, by that mechanism, to enhance BDNF signalling [49,50]. However,
609 preliminary experiments showed that JIP3 and JIP4 association to Rab10 organelles is extremely low in
610 hippocampal neurons and does not respond to BDNF stimulation (see Supplementary Figure 2). Whether
611 LRRK2-mediated phosphorylation of Rab10 regulates the interaction with KIF13B is part of our ongoing
612 research efforts and will not be discussed here in detail; however, it is worth mentioning that all three Rab10,
613 KIF13B and LRRK2 have been implicated in the formation of tubular endosomes [29,51]. Among the most
614 interesting candidates linking BDNF-signalling and LRRK2 activity is Vps35, a component of the retromer
615 complex that has been shown to modulate LRRK2 [52] and is recruited by TrkB binding to SorLA [53], a member of
616 the sortilin family. On the other hand, activation of Akt has been shown to compensate impairments of the
617 insulin-stimulated GLUT4 trafficking associated with LRRK2 deficiency [54], opening the possibility that other
618 downstream kinases could regulate Rab10 by LRRK2-independent mechanisms.
619
620 Once internalised, axonal TrkB reaches early endosomes, from where it can either recycle back to the plasma
621 membrane, thus fine-tuning the response of nerve terminals to BDNF (reviewed in [55]), or undergo sorting to
622 the retrograde axonal transport route, propagating neurotrophic signals to the soma [9,12,13]. Given that Rab10
623 downregulation decreased retrograde transport of TrkB and stimulation with BDNF promoted anterograde

transport of Rab10, we reasoned that Rab10 delivery to axon terminals facilitated the sorting of TrkB to retrogradely transported organelles. We demonstrated that Rab10DN expression increases the accumulation of internalised TrkB in early endosomes without significantly affecting recycling (Figure 5), thus indicating that functional Rab10 aids the exit of TrkB from early endosomes and its sorting to distinct axonal organelles.

When overexpressed, Rab10 is found at detectable levels in retrograde signalling endosomes positive for TrkB or $p75^{NTR}$ (Figure 4). An interesting observation is that only p75 receptors are present in Rab10-containing anterograde organelles, which bears the question on the role of the anterograde delivery of $p75^{NTR}$ to the distal axon. In sympathetic neurons, it has been shown that $p75^{NTR}$ is rapidly mobilised to the plasma membrane upon stimulation with NGF, depending on the activation of Arf6 [56], a small GTPase that has been shown to share common organelles with Rab10 in *C. elegans*[57].

At endogenous levels of Rab10, however, when we analysed triple co-localisation of internalised H_CT and TrkB with endogenous Rab10, we found that the absolute amount of retrograde TrkB associated to Rab10 organelles remains low (Figure 3e), suggesting that this interaction is transient. This is in line with previous evidence showing that in MDCK cells, Rab10 mediates transport from early endosomes to a polarised trafficking route [27]. Moreover, in *C. elegans,* Rab10 is recruited to early endosomes where it downregulates Rab5, helping to select cargoes for delivery to recycling endosomes [58]. According to this model, the transfer of TrkB from a stationary early endosome to a retrograde carrier would be preceded by a local increase of Rab10. In Figure 8b we show an example of a live-cell imaging experiment in which a TrkB-positive endosome makes this transition from stationary to retrograde. We show the level of Rab10-EGFP during the stationary phase (red), in the transition phase immediately preceding movement (yellow), and during processive retrograde transport (green). Crucially, Rab10 is recruited to this TrkB-positive axonal organelle few seconds before it starts moving retrogradely, strengthening the validity of our working model (Figure 8). Rab10 has been shown to participate in the biogenesis of tubular endosomes in mammalian cells [29] and regulates endosomal phosphatidylinositol-4,5-bisphosphate in *C. elegans,* suggesting that this small GTPase modulates the membrane recruitment of factors altering membrane curvature and budding [57]. During our live-cell imaging experiments, we observed Rab10-positive tubular organelles moving rapidly into proximal neurites, confirming that these structures are also generated in hippocampal neurons (see Supplementary Video 3). Interestingly, one of the well characterised roles of KIF13B in the brain is the transport of phosphatidylinositol-3,4,5-biphosphate via its interactor centaurin-alpha [59], which is essential for axon specification [60]. Further

research on the cargo content of Rab10 organelles in hippocampal neurons, including proteins and phospholipids, is warranted.

Our data suggests that Rab10 regulates the amount of internalised TrkB that is sorted to retrograde signalling endosomes in response to the concentration of BDNF at axon terminals. Since BDNF is known to be released post-synaptically as a function of neuronal activity [61], retrograde neurotrophic signalling from the axon

Figure 8. Model: Role of Rab10 in the sorting of TrkB to retrograde axonal transport.

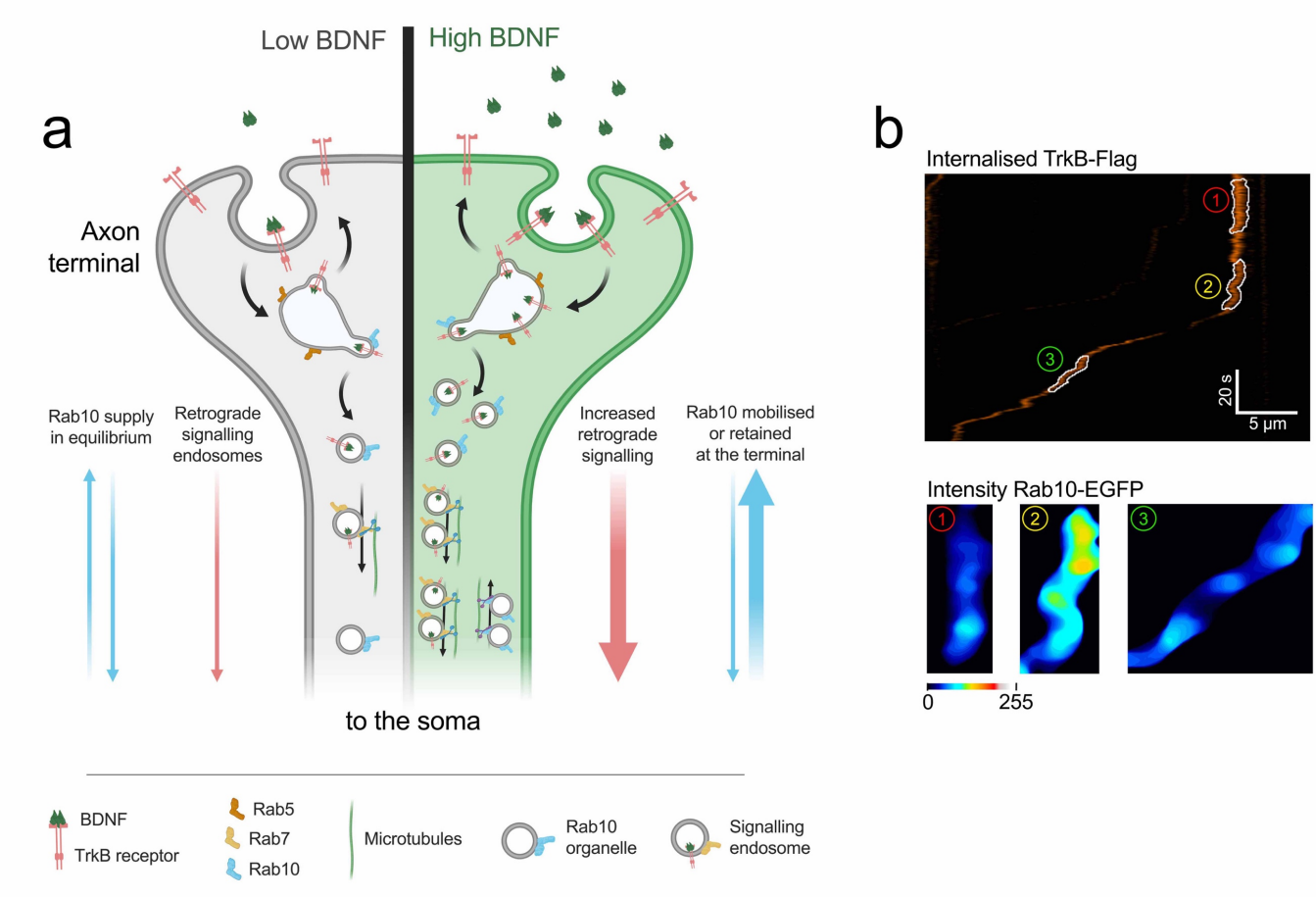

(a) At steady state, low concentrations of BDNF (grey side of the terminal) induce basal levels of TrkB internalisation. Rab10 supply (blue arrows) is in equilibrium and it mediates a baseline level of TrkB retrograde transport (pink arrows). Upon increase of BDNF (green side of the axon terminal), TrkB endocytosis as well as the proportion of Rab10 organelles moving towards the axon terminal are increased. Increased amounts of Rab10 result in further facilitation of the sorting of TrkB out of early endosome and an augmented flow of retrograde signalling carriers. **(b)** This model predicts that the transition from stationary early endosomes to processive retrograde carriers would be preceded by the focal recruitment of Rab10. The top panel shows an example of a kymograph of internalised TrkB-Flag in the axon. In the kymograph, three segments have been highlighted: 1 - stationary phase, 2 - transition phase, 3 - retrograde transport phase. The bottom panel shows the levels of Rab10-EGFP in these segments, which clearly demonstrates the enhanced recruitment of Rab10 during the transition phase, before onset of transport .

675 terminal is a substantial feedback mechanism regulating growth and survival, and therefore, ensuring that the
676 active circuit is preserved. To keep this feedback signal meaningful, any change in the availability of BDNF at
677 the synapse must translate into proportional changes in the intensity of the signal arriving at the soma. We
678 propose that Rab10 organelles deliver crucial components of the sorting machinery on demand. At steady
679 state, the anterograde and retrograde flow of Rab10 organelles is in equilibrium (Fig 8; *low BDNF*). Further
680 decrease in BDNF concentration makes retrograde transport of Rab10 compartments predominant, as
681 observed in live-cell imaging experiments performed in neurons treated with anti-BDNF blocking antibodies
682 (Figure 4, no BDNF). In contrast, adding BDNF reverts the directional bias of Rab10 organelles to anterograde
683 Fig 8; *high BDNF*), which allows the delivery of appropriate levels of the sorting machinery to nerve terminals,
684 thus increasing the efficiency of TrkB retrograde transport.
685
686 An independent example of anterograde delivery of components for the sorting of retrograde signalling
687 molecules has been hypothesised for the bone-morphogenetic protein (BMP) pathway in *Drosophila* motor
688 neurons. In this work, Khc-73, the fly orthologue of KIF13B, has been shown to regulate BMP sorting from
689 early endosomes at the neuromuscular junction [62]. This suggest that the proposed mechanism is evolutionary
690 conserved in different neuronal types, increasing its potential as a therapeutic target for pathologies in which
691 neurotrophic signalling from distal axons is impaired.
692
693 Little is known about the specific sorting machinery required for the biogenesis of signalling endosomes.
694 Endophilins A1 and A3 have been shown to regulate the trafficking of TrkB across early endosomes and
695 mediate survival signalling [14,63]. Interestingly, LRRK2 substrates include endophilin A1 as well as Rab10,
696 opening the possibility of both being found on the same organelle [64]. Moreover, KIF13B has also been found
697 to be enriched in early endosomes [65]. Further identification of components of the sorting machinery delivered
698 to axonal terminals by Rab10-positive carriers will be crucial to understand not only how this mechanism
699 allows coordination between local signalling and global neuronal responses, but also how this process may fail
700 in neurodegeneration. In this light, promoting the delivery of Rab10 organelles to nerve terminals may be
701 explored as an innovative therapeutic strategy for diseases in which the endo-lysosomal system is overloaded
702 or dysfunctional, such as Alzheimer's disease [66,67], or to increase the ability of axons to respond to trophic
703 factors during regeneration.
704
705
706

707 # Materials and methods
708

709 *Key resources table*

REAGENT or RESOURCE	SOURCE	IDENTIFIER
Antibodies		
Goat anti-Rab10	Santa Cruz Biotechnologies	Cat#sc-6564, RRID:AB_2237844
Mouse anti-Rab10	Abcam	Cat#ab104859, RRID:AB_10711207
Rabbit anti-Rab10	Cell Signalling	Cat#8127, RRID:AB_10828219
Rabbit anti-TrkB	Merck (Millipore)	Cat#AB9872, RRID:AB_11214317
Chicken anti-Tubulin ßIII	Synaptic Systems	Cat#302 306, RRID:AB_2620048
Rabbit anti-phosphorylated CREB	Abcam	Cat#ab32096, RRID:AB_731734
Mouse anti-Rab7	Abcam	Cat#ab50533, RRID:AB_882241
Rabbit anti-Rab5	Abcam	Cat#ab13253, RRID:AB_299796
Rabbit anti-KIF13B	Bioss	Cat#bs-12387R, RRID:AB_2895287
Rabbit anti-KIF5B	Abcam	Cat#ab5629, RRID:AB_2132379
Mouse anti-GFP (B-2)	Santa Cruz Biotechnologies	Cat#sc-9996, RRID: AB_627695
Mouse anti-HA (12CA5)	Cancer Research UK	Cat#12CA5, RRID:AB_2920713
Mouse anti-Flag (M1)	Sigma	Cat#F3040, RRID:AB_439712
Rabbit anti-p75NTR	Cancer Research UK	Cat#CRD5410, RRID:AB_2864325
Recombinant DNA		
TET ON Advance	Takara Bio (Clontech)	Cat#630930
pLVX shRab10	this study	-
pLVX Rab10 myc	this study	-
pEGFP-C1	Clontech	*discontinued*
Rab10 WT EGFP	Marci Scidmore lab	RRID:Addgene_49472
Rab10 T23N EGFP	Marci Scidmore lab	RRID:Addgene_49545
Rab10 WT HA	MRC Protein Phosphorylation and Ubiquitylation Unit (Dario Alessi)	DU44250
KIF13B GFP	Marvin Bentley lab	RRID:Addgene_134626
TrkB-FLAG	Francis Lee lab	-

710

711 *Neuronal cultures*

712 Embryonic hippocampal neurons from C57BL/6 mice of either sex and embryonic age of 16-17 days where
713 dissected adapting previously described protocols [68]. Dissection was performed in cold Hanks' balanced salt
714 solution (HBSS) and the tissue was collected in cold Hibernate E medium (ThermoFisher, #A1247601). After
715 incubating for 10 minutes in 300 µL of Accumax (Innovative Cell Technologies, #AM105) diluted in HBSS (1:1),
716 tissue was washed in HBSS, resuspended in warm plating medium (Minimum Essential Medium supplemented
717 with 10% horse serum, 6% glucose and 2 mM glutamine) and mechanically dissociated by pipetting. 10,000-
718 12,000 neurons per cm^2 were then seeded on glass coverslips or microfluidic chambers, pre-coated with 1
719 mg/mL poly-L-lysine. Before coating, glass coverslips were treated overnight with NoChromix (Godax
720 Laboratories), washed three times and sterilised in 70% ethanol. Microfluidic chambers were produced in-
721 house as previously described [69,70]. Polydimethylsiloxane inserts were fabricated from resin moulds, which are
722 replicas of the master template produced by soft lithography, and then irreversibly bound to glass-bottom
723 dishes (WillCo Wells, #HBSB-3512) by plasma treatment. Neurons were left in plating medium for 1.5 h and
724 then shifted to maintenance medium (Neurobasal supplemented with B27, 2 mM glutamine, 6% glucose and
725 antibiotics). Half of the culture medium was replaced by fresh medium every 3-4 days.

726

727 *Immunofluorescence.*

728 Cells were washed in phosphate buffer saline (PBS) and fixed for 15 min in 3% paraformaldehyde (PFA) and
729 4% sucrose dissolved in PBS. Next, they were incubated in 0.15 M glycine dissolved in PBS for 10 minutes and
730 then blocked and permeabilised simultaneously by incubation in 5% bovine serum albumin (BSA) and 0.1%
731 saponin in PBS for 1 hour. Samples were incubated at 4˚C overnight with primary antibodies diluted in 5% BSA,
732 0.05% saponin, 0.1 mM $CaCl_2$ and 0.1 mM $MgCl_2$ dissolved in PBS at the following concentrations: 1:50 goat
733 anti-Rab10 (Santa Cruz Biotechnologies, cat no. sc-6564, RRID:AB_2237844); 1:200 mouse anti-Rab10 (Abcam,
734 cat no. ab104859, RRID:AB_10711207); 1:200 rabbit anti-Rab10 (Cell Signalling Technology, cat no. 8127,
735 RRID:AB_10828219); 1:300 chicken anti-ßIII tubulin (Synaptic Systems, cat no. 302 306, AB_2620048); 1:250
736 rabbit anti-phosphorylated CREB S133 (Abcam, cat no. ab32096, RRID:AB_731734); 1:200 mouse anti-Rab7
737 (Abcam, cat no. ab50533, RRID:AB_882241); and 1:200 rabbit anti-Rab5 (Abcam, cat no. ab13253,
738 RRID:AB_299796). Then, cells were washed three times with PBS and incubated for 90 minutes with
739 AlexaFluor-conjugated secondary antibodies 1:400 (ThermoFisher) in 5% BSA, 0.05% saponin, 0.1 mM $CaCl_2$
740 and 0.1 mM $MgCl_2$ dissolved in PBS. 4',6-diamidino-2-phenylindole (DAPI) was added with the secondary
741 antibodies when appropriate. Finally, coverslips were washed in PBS and mounted with Mowiol.

742

743 *Rab10 knockdown*

744 Rab10 was knocked down by transducing 5 DIV hippocampal neurons with an inducible shRNA Rab10 lentivirus
745 (pTightPuro-shRNA Rab10) and its doxycycline-dependent regulator TET-ON Advance. After 48 hours they
746 were treated with doxycycline 1 µg/mL and kept in the incubator for 12, 18, 24, 36 and 48 hours. Cell density,
747 levels of Rab10 and TrkB, as well as the general health of the culture were analysed at 12, 24 and 48 hours to
748 establish the optimal time frame for the following experiments.

749

750 *Transfection and plasmids*

751 Hippocampal neurons were transfected at 7 days in vitro (DIV) using Lipofectamine 2000 (Thermo Fisher, Cat.
752 no. 11668019). Experiments were carried out after 20-24 hours. The pEGFP-C1 plasmid is from Clontech
753 (Addgene plasmid # 13031, RRID:Addgene_13031), the plasmids for Rab10 WT EGFP (RRID:Addgene_49472)
754 and Rab10 T23N EGFP (RRID:Addgene_49545) were a gift from Marci Scidmore [71], TrkB-FLAG plasmid was a
755 gift from Francis Lee [31]. Neuro-2a cells were transfected using Lipofectamine 3000 (Thermo Fisher, Cat. no.
756 L3000001) and the experiments were done 48 hours later. The KIF13B-GFP plasmid (RRID:Addgene_134626)
757 was a gift from Marvin Bentley [25], whilst the Rab10-HA plasmid was provided by Dario Alessi and Miratul Muqit
758 (Dundee University, DU44250).

759

760 *Retrograde accumulation and signalling assays*

761 Hippocampal neurons were seeded in custom-made microfluidic devices and after 5 DIV they were transduced
762 with the inducible shRNA Rab10 and TET-ON Advance lentiviruses. At 7 DIV, dishes with overt axon crossing
763 were selected and doxycycline 1 µg/mL was added to the cell bodies, 18-22 hours later the media was replaced
764 with Neurobasal in somatic and axonal compartments to deplete cells from endogenous growth factors for 1
765 hours. For analysing the retrograde accumulation of TrkB, we added polyclonal antibodies against the
766 extracellular domain of TrkB (1:50 rabbit anti-TrkB, Millipore, cat no. AB9872, RRID:AB_2236301) together
767 with 20 ng/mL BDNF for 2.5 hours. After PFA fixation, the transport of internalized antibodies was revealed by
768 incubating the somatic compartment with fluorescently-labelled secondary antibodies. The same protocol was
769 used to study retrograde propagation of neurotrophic signalling; after 1 hour of growth factor-depletion,
770 axons were stimulated with 20 ng/mL BDNF for 2.5 hours and after fixation, phosphorylation of CREB in the
771 nucleus was analysed by immunofluorescence.

772

773 *Co-localisation studies*

774 To analyse the presence of two markers in the same organelle, we used confocal z-stack images (voxel size:
775 0.197 x 0.197 x 0.5 µm) and the confined displacement algorithm to measure Manders' correlation index
776 within axons and determine its statistical significance compared to random images of identical total intensity
777 and shape [20]. To compute random scenarios, seven random radial displacements were taken at a maximum
778 radial distance of 12 pixels (a total of 353 samples), and histograms binning = 16. CDA was implemented by
779 using the plugin from the GDSC University of Sussex
780 (http://www.sussex.ac.uk/gdsc/intranet/microscopy/UserSupport/AnalysisProtocol/imagej/colocalisation).
781 All the data points were plotted and the mean and standard error is indicated for each group and compared
782 using Student t-test. Statistical significance of the individual data point is colour coded (see figure legends).
783
784 *Super-resolution radial fluctuations*
785 High-fidelity super-resolution information was extracted from time series of 1,000 confocal images per
786 channel by using super-resolution radial fluctuations (SRRF) algorithm [72]. Super-resolution images were then
787 quality-controlled by using Super-Resolution Quantitative Image Rating and Reporting of Error Locations
788 (SQUIRREL) algorithm [73]. Implementation of the algorithms was done in FIJI by using the open-source plugin
789 NanoJ-core (https://henriqueslab.github.io/resources/NanoJ).
790
791 *Immunoendocytosis*
792 Hippocampal neurons transfected with TrkB-Flag were kept in Neurobasal media for 1 hour and then
793 incubated on ice with 1:50 mouse anti-Flag antibody (Sigma-Aldrich Cat no. F3040, RRID:AB_439712). In
794 selected samples, 20 nM H_CT was also added [12]. Internalisation of receptors was then induced by incubation
795 with 50 ng/mL BDNF for 30 minutes at 37˚C . Antibodies bound to receptors still at the cell surface were
796 dissociated by washing twice for 1 minute in PBS supplemented with 1 mM EDTA. In experiments to measure
797 recycling of internalised receptors, neurons were further stimulated with BDNF for other 60 minutes in the
798 presence of an AlexaFluor647-conjugated anti-mouse secondary antibody, fixed, permeabilised and incubated
799 with an AlexaFluor555-conjugated anti-mouse secondary antibody to detect total internalised receptor.
800
801 *Axonal transport*
802 Axonal transport of overexpressed fluorescent proteins and internalised fluorescent antibodies was analysed
803 from confocal time series of 1 frame/s and a pixel size of ~0.1 x 0.1 μm^2, captured during 5 minutes intervals
804 at different time points by using a Zeiss LSM 780 NLO multiphoton confocal microscope with an oil immersion
805 63× objective and equipped with an environmental chamber (Zeiss XL multi S1 DARK LS set at 37˚C and

806 environmental CO_2). For these experiments, neurons were cultured on 25 mm coverslips kept in Neurobasal
807 for 1 hour prior to cell imaging and mounted inside Attofluor chambers (Thermo-Fisher Scientific, Cat no.
808 A7816) with BrightCell NEUMO photostable media (Sigma-Aldrich, Cat no. SCM145) supplemented with 10
809 mM HEPES. Speed, pausing and direction of labelled organelles were analysed from kymographs by using
810 Kymoanalyzer set of macros from Encalada lab (https://www.encalada.scripps.edu/kymoanalyzer) [74].
811
812 *Co-immunoprecipitation*
813 Neuro-2A cells stably expressing TrkB-Flag [26] and transfected with plasmids encoding Rab10-HA and KIF13B-
814 GFP were starved for 1 hour, stimulated or not with BDNF for 30 minutes at 37˚C and then scrapped and
815 incubated at 4˚C for 30 minutes in lysis buffer containing 25 mM 4-morpholine-propanesulfonic acid sodium
816 salt (MOPS) pH 7.2, 100 mM KCl, 10 mM $MgCl_2$, 1% octyl-phenoxy-polyethoxyethanol (IGEPAL CA-630, Sigma-
817 Aldrich, Cat. no. I3021) and HALT proteases and phosphatases inhibitor (Thermo Fisher, Cat. no. 78425). After
818 clearing by centrifugation at 21,000 *g* for 10 minutes, the detergent concentration was adjusted to 0.5%. Pre-
819 washed anti-HA magnetic beads (Pierce, Cat. no. 88837) were incubated with lysates overnight at 4˚C. Samples
820 were washed in lysis buffer 5 times and elutes in loading buffer (NuPAGE LDS sample buffer, Thermo Fisher,
821 Cat. no. NP0007, supplemented with 50 mM DTT) at 95˚C for 10 minutes. The levels of immunoprecipitated
822 Rab10 and KIF13B were analysed by western blot using mouse anti-HA (Cancer Research UK, Cat. no. 12CA5,
823 RRID:AB_2920713) and mouse anti-GFP B-2 (Santa Cruz Biotechnologies, Cat. no. sc-9996, RRID:AB_627695)
824 antibodies.
825
826 *Statistical Analysis*
827 Data generated in independent experiments were tested for normality and homoscedasticity to apply the
828 appropriate corrections to the statistical tests. Each specific test, its degrees of freedom and level of
829 significance are indicated in the respective figure legend. Further details are summarised in the statistical
830 annex (Supplementary Table 1). Plots show mean ± standard error and exact p values are indicated when
831 relevant.
832
833 *Software*
834 Images were handled, edited and analysed using ImageJ/FIJI (version 2.1.0, 1.53c). Figures were checked with
835 Coblis (https://www.color-blindness.com/coblis-color-blindness-simulator/), using The Colour Blind Simulator
836 algorithms from Matthew Wickline and the Human-Computer Interaction Resource Network. Palettes were
837 adjusted to maximise visibility. The Orange/Green/Purple balanced look-up table was obtained from

838 Christophe Leterrier's GitHub repository (https://github.com/cleterrier/ChrisLUTs). Data were imported,
839 analysed and sorted as R files using RStudio (version 1.0.44). GraphPad Prism for Mac (version 6.00, GraphPad
840 Software) was used for running statistical analysis and generate the plots included in the figures. Illustrations
841 were created with BioRender (http://www.biorender.com). Updated versions of ImageJ macros and R scripts
842 used in this article, as well as the specific implementation of Kymoanalyzer used to analyse our datasets, can
843 be found on our GitHub repository (https://github.com/omlazo).
844

845 ## Acknowledgements

846 We thank Dr James N Sleigh (UCL Queen Square Institute of Neurology) for critical reading of the manuscript.
847 This work was supported by the MRC Project grant MR/T001976/1 [OL], the Wellcome Trust Senior
848 Investigator Awards (107116/Z/15/Z and and 223022/Z/21/Z) [GS] and the UK Dementia Research Institute
849 Foundation award UKDRI-1005 [GS].
850

851 ## Author's contributions

852 OL performed the research and drafted the manuscript, which was revised by GS. OL and GS interpreted the
853 data and approved the submission of this work.
854

855 ## Conflict of Interest

856 The authors have no competing interest to declare.
857

858 ## References

859 1 Andres-Alonso, M. *et al.* SIPA1L2 controls trafficking and local signaling of TrkB-containing
860 amphisomes at presynaptic terminals. *Nat Commun* **10**, 5448, doi:10.1038/s41467-019-13224-z
861 (2019).
862 2 Szobota, S. *et al.* BDNF, NT-3 and Trk receptor agonist monoclonal antibodies promote neuron
863 survival, neurite extension, and synapse restoration in rat cochlea ex vivo models relevant for hidden
864 hearing loss. *PLoS One* **14**, e0224022, doi:10.1371/journal.pone.0224022 (2019).
865 3 Woo, D. *et al.* Locally Activating TrkB Receptor Generates Actin Waves and Specifies Axonal Fate. *Cell*
866 *Chem Biol* **26**, 1652-1663 e1654, doi:10.1016/j.chembiol.2019.10.006 (2019).
867 4 Barford, K., Deppmann, C. & Winckler, B. The neurotrophin receptor signaling endosome: Where
868 trafficking meets signaling. *Dev Neurobiol* **77**, 405-418, doi:10.1002/dneu.22427 (2017).
869 5 Villarroel-Campos, D., Schiavo, G. & Lazo, O. M. The many disguises of the signalling endosome. *FEBS*
870 *Lett* **592**, 3615-3632, doi:10.1002/1873-3468.13235 (2018).
871 6 Du, J. L. & Poo, M. M. Rapid BDNF-induced retrograde synaptic modification in a developing
872 retinotectal system. *Nature* **429**, 878-883, doi:10.1038/nature02618 (2004).

7 Pazyra-Murphy, M. F. *et al.* A retrograde neuronal survival response: target-derived neurotrophins regulate MEF2D and bcl-w. *J Neurosci* **29**, 6700-6709, doi:10.1523/JNEUROSCI.0233-09.2009 (2009).

8 Watson, F. L. *et al.* Rapid nuclear responses to target-derived neurotrophins require retrograde transport of ligand-receptor complex. *J Neurosci* **19**, 7889-7900 (1999).

9 Zhou, B., Cai, Q., Xie, Y. & Sheng, Z. H. Snapin recruits dynein to BDNF-TrkB signaling endosomes for retrograde axonal transport and is essential for dendrite growth of cortical neurons. *Cell Rep* **2**, 42-51, doi:10.1016/j.celrep.2012.06.010 (2012).

10 Huang, E. J. & Reichardt, L. F. Trk receptors: roles in neuronal signal transduction. *Annu Rev Biochem* **72**, 609-642, doi:10.1146/annurev.biochem.72.121801.161629 (2003).

11 Minichiello, L. TrkB signalling pathways in LTP and learning. *Nat Rev Neurosci* **10**, 850-860, doi:10.1038/nrn2738 (2009).

12 Deinhardt, K. *et al.* Rab5 and Rab7 control endocytic sorting along the axonal retrograde transport pathway. *Neuron* **52**, 293-305, doi:10.1016/j.neuron.2006.08.018 (2006).

13 Ha, J. *et al.* A neuron-specific cytoplasmic dynein isoform preferentially transports TrkB signaling endosomes. *J Cell Biol* **181**, 1027-1039, doi:10.1083/jcb.200803150 (2008).

14 Burk, K. *et al.* EndophilinAs regulate endosomal sorting of BDNF-TrkB to mediate survival signaling in hippocampal neurons. *Sci Rep* **7**, 2149, doi:10.1038/s41598-017-02202-4 (2017).

15 Kucharava, K. *et al.* Sodium-hydrogen exchanger 6 (NHE6) deficiency leads to hearing loss, via reduced endosomal signalling through the BDNF/Trk pathway. *Sci Rep* **10**, 3609, doi:10.1038/s41598-020-60262-5 (2020).

16 Bucci, C., Alifano, P. & Cogli, L. The role of rab proteins in neuronal cells and in the trafficking of neurotrophin receptors. *Membranes (Basel)* **4**, 642-677, doi:10.3390/membranes4040642 (2014).

17 Deng, C. Y. *et al.* JIP1 mediates anterograde transport of Rab10 cargos during neuronal polarization. *J Neurosci* **34**, 1710-1723, doi:10.1523/JNEUROSCI.4496-13.2014 (2014).

18 Debaisieux, S., Encheva, V., Chakravarty, P., Snijders, A. P. & Schiavo, G. Analysis of Signaling Endosome Composition and Dynamics Using SILAC in Embryonic Stem Cell-Derived Neurons. *Mol Cell Proteomics* **15**, 542-557, doi:10.1074/mcp.M115.051649 (2016).

19 Gonzalez-Gutierrez, A., Lazo, O. M. & Bronfman, F. C. The Rab5-Rab11 Endosomal Pathway is Required for BDNF-Induced CREB Transcriptional Regulation in Hippocampal Neurons. *J Neurosci* **40**, 8042-8054, doi:10.1523/JNEUROSCI.2063-19.2020 (2020).

20 Ramirez, O., Garcia, A., Rojas, R., Couve, A. & Hartel, S. Confined displacement algorithm determines true and random colocalization in fluorescence microscopy. *J Microsc* **239**, 173-183, doi:10.1111/j.1365-2818.2010.03369.x (2010).

21 Goto-Silva, L. *et al.* Retrograde transport of Akt by a neuronal Rab5-APPL1 endosome. *Sci Rep* **9**, 2433, doi:10.1038/s41598-019-38637-0 (2019).

22 Zhen, Y. & Stenmark, H. Cellular functions of Rab GTPases at a glance. *J Cell Sci* **128**, 3171-3176, doi:10.1242/jcs.166074 (2015).

23 Guillaud, L., El-Agamy, S. E., Otsuki, M. & Terenzio, M. Anterograde Axonal Transport in Neuronal Homeostasis and Disease. *Front Mol Neurosci* **13**, 556175, doi:10.3389/fnmol.2020.556175 (2020).

24 Kwan, A. C., Dombeck, D. A. & Webb, W. W. Polarized microtubule arrays in apical dendrites and axons. *Proc Natl Acad Sci U S A* **105**, 11370-11375, doi:10.1073/pnas.0805199105 (2008).

25 Yang, R. *et al.* A novel strategy to visualize vesicle-bound kinesins reveals the diversity of kinesin-mediated transport. *Traffic* **20**, 851-866, doi:10.1111/tra.12692 (2019).

26 Terenzio, M. *et al.* Bicaudal-D1 regulates the intracellular sorting and signalling of neurotrophin receptors. *EMBO J* **33**, 1582-1598, doi:10.15252/embj.201387579 (2014).

27 Babbey, C. M. *et al.* Rab10 regulates membrane transport through early endosomes of polarized Madin-Darby canine kidney cells. *Mol Biol Cell* **17**, 3156-3175, doi:10.1091/mbc.e05-08-0799 (2006).

28 Brewer, P. D., Habtemichael, E. N., Romenskaia, I., Mastick, C. C. & Coster, A. C. Glut4 Is Sorted from a Rab10 GTPase-independent Constitutive Recycling Pathway into a Highly Insulin-responsive Rab10 GTPase-dependent Sequestration Pathway after Adipocyte Differentiation. *J Biol Chem* **291**, 773-789, doi:10.1074/jbc.M115.694919 (2016).

29 Etoh, K. & Fukuda, M. Rab10 regulates tubular endosome formation through KIF13A and KIF13B motors. *J Cell Sci* **132**, doi:10.1242/jcs.226977 (2019).

30 Xu, X. H. *et al.* MARCKS regulates membrane targeting of Rab10 vesicles to promote axon development. *Cell Res* **24**, 576-594, doi:10.1038/cr.2014.33 (2014).

31 Chen, Z. Y., Ieraci, A., Tanowitz, M. & Lee, F. S. A novel endocytic recycling signal distinguishes biological responses of Trk neurotrophin receptors. *Mol Biol Cell* **16**, 5761-5772, doi:10.1091/mbc.e05-07-0651 (2005).

32 Wang, H., Xu, J., Lazarovici, P., Quirion, R. & Zheng, W. cAMP Response Element-Binding Protein (CREB): A Possible Signaling Molecule Link in the Pathophysiology of Schizophrenia. *Front Mol Neurosci* **11**, 255, doi:10.3389/fnmol.2018.00255 (2018).

33 Esvald, E. E. *et al.* CREB Family Transcription Factors Are Major Mediators of BDNF Transcriptional Autoregulation in Cortical Neurons. *J Neurosci* **40**, 1405-1426, doi:10.1523/JNEUROSCI.0367-19.2019 (2020).

34 Kwon, M., Fernandez, J. R., Zegarek, G. F., Lo, S. B. & Firestein, B. L. BDNF-promoted increases in proximal dendrites occur via CREB-dependent transcriptional regulation of cypin. *J Neurosci* **31**, 9735-9745, doi:10.1523/JNEUROSCI.6785-10.2011 (2011).

35 Cohen, M. S., Bas Orth, C., Kim, H. J., Jeon, N. L. & Jaffrey, S. R. Neurotrophin-mediated dendrite-to-nucleus signaling revealed by microfluidic compartmentalization of dendrites. *Proc Natl Acad Sci U S A* **108**, 11246-11251, doi:10.1073/pnas.1012401108 (2011).

36 Riccio, A., Pierchala, B. A., Ciarallo, C. L. & Ginty, D. D. An NGF-TrkA-mediated retrograde signal to transcription factor CREB in sympathetic neurons. *Science* **277**, 1097-1100, doi:10.1126/science.277.5329.1097 (1997).

37 Lazo, O. M. *et al.* BDNF regulates Rab11-mediated recycling endosome dynamics to induce dendritic branching. *J Neurosci* **33**, 6112-6122, doi:10.1523/JNEUROSCI.4630-12.2013 (2013).

38 Moya-Alvarado, G., Gonzalez, A., Stuardo, N. & Bronfman, F. C. Brain-Derived Neurotrophic Factor (BDNF) Regulates Rab5-Positive Early Endosomes in Hippocampal Neurons to Induce Dendritic Branching. *Front Cell Neurosci* **12**, 493, doi:10.3389/fncel.2018.00493 (2018).

39 Chua, C. E. L. & Tang, B. L. Rab 10-a traffic controller in multiple cellular pathways and locations. *J Cell Physiol* **233**, 6483-6494, doi:10.1002/jcp.26503 (2018).

40 Taylor, C. A., Yan, J., Howell, A. S., Dong, X. & Shen, K. RAB-10 Regulates Dendritic Branching by Balancing Dendritic Transport. *PLoS Genet* **11**, e1005695, doi:10.1371/journal.pgen.1005695 (2015).

41 Hirokawa, N. & Tanaka, Y. Kinesin superfamily proteins (KIFs): Various functions and their relevance for important phenomena in life and diseases. *Exp Cell Res* **334**, 16-25, doi:10.1016/j.yexcr.2015.02.016 (2015).

42 Soppina, V. *et al.* Dimerization of mammalian kinesin-3 motors results in superprocessive motion. *Proc Natl Acad Sci U S A* **111**, 5562-5567, doi:10.1073/pnas.1400759111 (2014).

43 Sano, H. *et al.* Rab10, a target of the AS160 Rab GAP, is required for insulin-stimulated translocation of GLUT4 to the adipocyte plasma membrane. *Cell Metab* **5**, 293-303, doi:10.1016/j.cmet.2007.03.001 (2007).

44 Xu, L., Nagai, Y., Kajihara, Y., Ito, G. & Tomita, T. The Regulation of Rab GTPases by Phosphorylation. *Biomolecules* **11**, doi:10.3390/biom11091340 (2021).

45 Pfeffer, S. R., Dirac-Svejstrup, A. B. & Soldati, T. Rab GDP dissociation inhibitor: putting rab GTPases in the right place. *J Biol Chem* **270**, 17057-17059, doi:10.1074/jbc.270.29.17057 (1995).

46 Waschbusch, D. *et al.* Structural Basis for Rab8a Recruitment of RILPL2 via LRRK2 Phosphorylation of Switch 2. *Structure* **28**, 406-417 e406, doi:10.1016/j.str.2020.01.005 (2020).

47 Cockburn, J. J. B. *et al.* Insights into Kinesin-1 Activation from the Crystal Structure of KLC2 Bound to JIP3. *Structure* **26**, 1486-1498 e1486, doi:10.1016/j.str.2018.07.011 (2018).

48 Isabet, T. *et al.* The structural basis of Arf effector specificity: the crystal structure of ARF6 in a complex with JIP4. *EMBO J* **28**, 2835-2845, doi:10.1038/emboj.2009.209 (2009).

49 Huang, S. H. *et al.* JIP3 mediates TrkB axonal anterograde transport and enhances BDNF signaling by directly bridging TrkB with kinesin-1. *J Neurosci* **31**, 10602-10614, doi:10.1523/JNEUROSCI.0436-11.2011 (2011).

50 Sun, T. *et al.* JIP1 and JIP3 cooperate to mediate TrkB anterograde axonal transport by activating kinesin-1. *Cell Mol Life Sci* **74**, 4027-4044, doi:10.1007/s00018-017-2568-z (2017).

51 Bonet-Ponce, L. *et al.* LRRK2 mediates tubulation and vesicle sorting from lysosomes. *Sci Adv* **6**, doi:10.1126/sciadv.abb2454 (2020).

52 Mir, R. *et al.* The Parkinson's disease VPS35[D620N] mutation enhances LRRK2-mediated Rab protein phosphorylation in mouse and human. *Biochem J* **475**, 1861-1883, doi:10.1042/BCJ20180248 (2018).

53 Rohe, M., Hartl, D., Fjorback, A. N., Klose, J. & Willnow, T. E. SORLA-mediated trafficking of TrkB enhances the response of neurons to BDNF. *PLoS One* **8**, e72164, doi:10.1371/journal.pone.0072164 (2013).

54 Funk, N. *et al.* The Parkinson's disease-linked Leucine-rich repeat kinase 2 (LRRK2) is required for insulin-stimulated translocation of GLUT4. *Sci Rep* **9**, 4515, doi:10.1038/s41598-019-40808-y (2019).

55 Andreska, T., Luningschror, P. & Sendtner, M. Regulation of TrkB cell surface expression-a mechanism for modulation of neuronal responsiveness to brain-derived neurotrophic factor. *Cell Tissue Res* **382**, 5-14, doi:10.1007/s00441-020-03224-7 (2020).

56 Hickman, F. E., Stanley, E. M. & Carter, B. D. Neurotrophin Responsiveness of Sympathetic Neurons Is Regulated by Rapid Mobilization of the p75 Receptor to the Cell Surface through TrkA Activation of Arf6. *J Neurosci* **38**, 5606-5619, doi:10.1523/JNEUROSCI.0788-16.2018 (2018).

57 Shi, A. & Grant, B. D. Interactions between Rab and Arf GTPases regulate endosomal phosphatidylinositol-4,5-bisphosphate during endocytic recycling. *Small GTPases* **4**, 106-109, doi:10.4161/sgtp.23477 (2013).

58 Liu, O. & Grant, B. D. Basolateral Endocytic Recycling Requires RAB-10 and AMPH-1 Mediated Recruitment of RAB-5 GAP TBC-2 to Endosomes. *PLoS Genet* **11**, e1005514, doi:10.1371/journal.pgen.1005514 (2015).

59 Hammonds-Odie, L. P. *et al.* Identification and cloning of centaurin-alpha. A novel phosphatidylinositol 3,4,5-trisphosphate-binding protein from rat brain. *J Biol Chem* **271**, 18859-18868, doi:10.1074/jbc.271.31.18859 (1996).

60 Horiguchi, K., Hanada, T., Fukui, Y. & Chishti, A. H. Transport of PIP3 by GAKIN, a kinesin-3 family protein, regulates neuronal cell polarity. *J Cell Biol* **174**, 425-436, doi:10.1083/jcb.200604031 (2006).

61 Matsuda, N. *et al.* Differential activity-dependent secretion of brain-derived neurotrophic factor from axon and dendrite. *J Neurosci* **29**, 14185-14198, doi:10.1523/JNEUROSCI.1863-09.2009 (2009).

62 Liao, E. H. *et al.* Kinesin Khc-73/KIF13B modulates retrograde BMP signaling by influencing endosomal dynamics at the Drosophila neuromuscular junction. *PLoS Genet* **14**, e1007184, doi:10.1371/journal.pgen.1007184 (2018).

63 Fu, X. *et al.* Retrolinkin cooperates with endophilin A1 to mediate BDNF-TrkB early endocytic trafficking and signaling from early endosomes. *Mol Biol Cell* **22**, 3684-3698, doi:10.1091/mbc.E11-04-0308 (2011).

64 Matta, S. *et al.* LRRK2 controls an EndoA phosphorylation cycle in synaptic endocytosis. *Neuron* **75**, 1008-1021, doi:10.1016/j.neuron.2012.08.022 (2012).

1014 65 Bentley, M., Decker, H., Luisi, J. & Banker, G. A novel assay reveals preferential binding between Rabs,
1015 kinesins, and specific endosomal subpopulations. *J Cell Biol* **208**, 273-281, doi:10.1083/jcb.201408056
1016 (2015).
1017 66 Van Acker, Z. P., Bretou, M. & Annaert, W. Endo-lysosomal dysregulations and late-onset Alzheimer's
1018 disease: impact of genetic risk factors. *Mol Neurodegener* **14**, 20, doi:10.1186/s13024-019-0323-7
1019 (2019).
1020 67 Xu, W., Fang, F., Ding, J. & Wu, C. Dysregulation of Rab5-mediated endocytic pathways in Alzheimer's
1021 disease. *Traffic* **19**, 253-262, doi:10.1111/tra.12547 (2018).
1022 68 Kaech, S. & Banker, G. Culturing hippocampal neurons. *Nat Protoc* **1**, 2406-2415,
1023 doi:10.1038/nprot.2006.356 (2006).
1024 69 Sannerud, R. *et al.* ADP ribosylation factor 6 (ARF6) controls amyloid precursor protein (APP)
1025 processing by mediating the endosomal sorting of BACE1. *Proc Natl Acad Sci U S A* **108**, E559-568,
1026 doi:10.1073/pnas.1100745108 (2011).
1027 70 Restani, L. *et al.* Botulinum neurotoxins A and E undergo retrograde axonal transport in primary motor
1028 neurons. *PLoS Pathog* **8**, e1003087, doi:10.1371/journal.ppat.1003087 (2012).
1029 71 Huang, B. *et al.* The Anaplasma phagocytophilum-occupied vacuole selectively recruits Rab-GTPases
1030 that are predominantly associated with recycling endosomes. *Cell Microbiol* **12**, 1292-1307,
1031 doi:10.1111/j.1462-5822.2010.01468.x (2010).
1032 72 Culley, S., Tosheva, K. L., Matos Pereira, P. & Henriques, R. SRRF: Universal live-cell super-resolution
1033 microscopy. *Int J Biochem Cell Biol* **101**, 74-79, doi:10.1016/j.biocel.2018.05.014 (2018).
1034 73 Culley, S. *et al.* Quantitative mapping and minimization of super-resolution optical imaging artifacts.
1035 *Nat Methods* **15**, 263-266, doi:10.1038/nmeth.4605 (2018).
1036 74 Neumann, S., Chassefeyre, R., Campbell, G. E. & Encalada, S. E. KymoAnalyzer: a software tool for the
1037 quantitative analysis of intracellular transport in neurons. *Traffic* **18**, 71-88, doi:10.1111/tra.12456
1038 (2017).
1039
1040

Supplementary material

TABLES

Supplementary Table 1 — Statistical summary

Figure		Variable	Test	Groups	Degrees of freedom	p value
1	b	Cells per field	two-way ANOVA	knock down; time; interaction	F(1,68)	0.0270; 0.0406; 0.2114
			Multiple comparisons	control : shRNA Rab10 at 24 h	t(68)	> 0.9999
			Multiple comparisons	control : shRNA Rab10 at 48 h	t(68)	0.0183
	c	Rab10 expression	two-way ANOVA	knock down; time; interaction	F(1,653); F(2,653); F(2,653)	< 0.0001
			Multiple comparisons	control : shRNA Rab10 at 12 h	t(653)	0.2012
			Multiple comparisons	control : shRNA Rab10 at 24 h	t(653)	< 0.0001
			Multiple comparisons	control : shRNA Rab10 at 48 h	t(653)	< 0.0001
2	d	TrkB accumulation	Unpaired t-Student	control : shRNA Rab10	t(140)	< 0.0001
	e	TrkB accumulation and Rab10 expression	Pearson r	control : shRNA Rab10	XY pairs= 131	< 0.0001
	g	pCREB abundance	one-way ANOVA	control, shRNA Rab10 and rescue	F(2,280)	< 0.0001
			Multiple comparisons	control : shRNA Rab10	t(280)	< 0.0001
			Multiple comparisons	control : rescue	t(280)	0.0336
3	b	Co-localisation Rab10 and Rab7	Unpaired t-Student	M1 control : BDNF	t(72.32)	0.0621
			Unpaired t-Student	M2 control : BDNF	t(62.33)	0.1043
	e	Area of overlay HcT and TrkB (retrograde TrkB)	one-way ANOVA	30, 60 and 90 mins	F(2,72)	< 0.0001
			Multiple comparisons	30 : 60 mins	t(72)	> 0.9999
			Multiple comparisons	60 : 90 mins	t(72)	0.0002
		Area of overlay retrograde TrkB and Rab10	one-way ANOVA	30, 60 and 90 mins	F(2,72)	0.2730
			Multiple comparisons	30 : 60 mins	t(72)	0.5717
			Multiple comparisons	60 : 90 mins	t(72)	> 0.9999
5	c	Direction of Rab10 organelles	Unpaired t-Student	Anterograde pre : post BDNF	t(14)	0.0150
			Unpaired t-Student	Retrograde pre : post BDNF	t(14)	0.0030
			Unpaired t-Student	Non-mobile pre : post BDNF	t(14)	0.4278
6	b	KIF13B intensity ratio	Kolmogorov-Smirnov t-Student	control : BDNF	t(79.5)	0.0177
	c	KIF13B area occupancy ratio	Kolmogorov-Smirnov t-Student	control : BDNF	t(79.5)	0.8024
	e	KIF5B intensity ratio	Kolmogorov-Smirnov t-Student	control : BDNF	t(62.5)	0.0644
	f	KIF5B area occupancy ratio	Kolmogorov-Smirnov t-Student	control : BDNF	t(62.5)	0.3738
	h	KIF13B co-immunoprecipitation	Paired t-Student	control : BDNF	t(6)	0.0024
7	c	Recycling of TrkB	Unpaired t-Student	EGFP : Rab10 DN	t(60.40)	0.3914
	e	Co-localisation TrkB and Rab5	Unpaired t-Student	EGFP : Rab10 DN	t(38.22)	0.0080

Supplementary Table 1: Summary of the statistical tests and their results for the data in the figures.

FIGURES

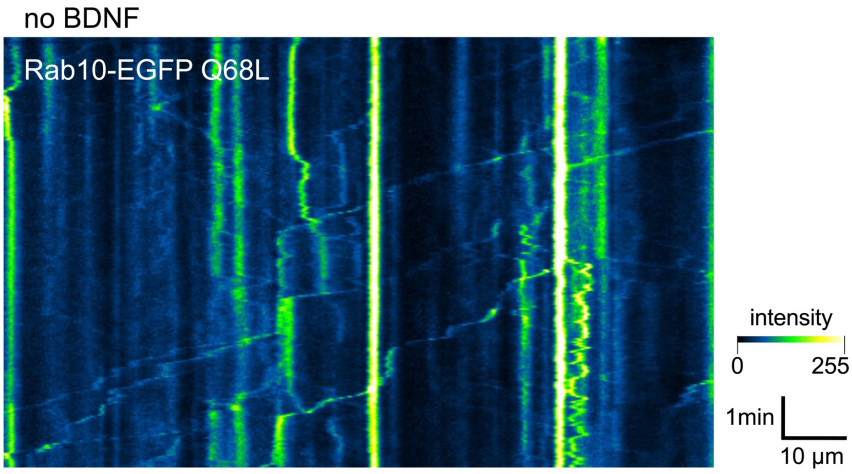

Supplementary Figure 1: Example of a kymograph showing the dynamics of the constitutively-active Rab10-EGFP Q68L mutant in a representative axon depleted of BDNF.

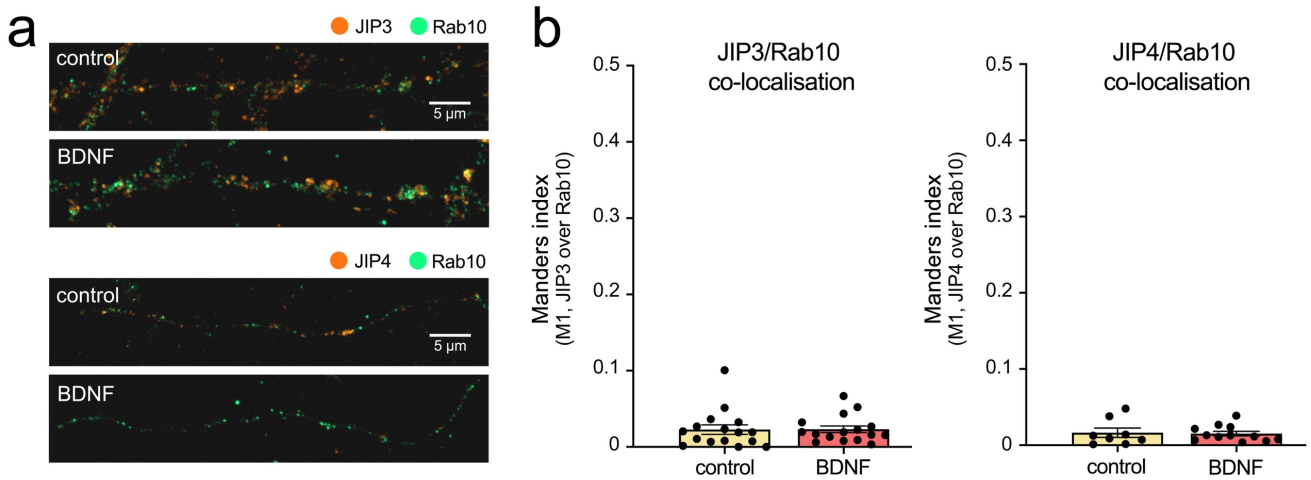

Supplementary Figure 2: Preliminary results showing **(a)** representative images of axons stained for Rab10 (green) and JIP3 or JIP4 (orange) and **(b)** Manders co-localisation coefficients for control versus BDNF-treated axons, showing that only ~2% of JIP3 or JIP4 is in Rab10 positive domains, with no change upon treatment with 50 ng/mL BDNF for 30 mins.

VIDEOS

https://www.dropbox.com/s/zq6bvvu0a8yrpyu/SV1%E2%80%94Rab10%20direction%20switch.mp4?dl=0
Supplementary Video 1: Representative axon in mass culture expressing Rab10-EGFP (with intensity colour-coded as in Figure 4a) before and after being stimulated with 50 ng/mL BDNF. Dimensions and speed are indicated in the video.

https://www.dropbox.com/s/l00rz2twzqr7mj8/SV2%E2%80%94Rab10%20picking%20up.mp4?dl=0
Supplementary Video 2: Representative time-lapse microscopy video of Rab10-EGFP (with intensity colour-coded as in Figure 4a) after 10 minutes upon stimulation with 50 ng/mL BDNF. A moving Rab10-positive organelle is indicated with a green arrowhead on the left, while in the centre a stationary organelle is indicated with a red arrowhead. The first endosome is moving anterogradely and when it runs next to the stationary organelle, they partially merge and continue moving. Dimensions and speed are indicated.

https://www.dropbox.com/s/fu0r5geri6rqugb/SV3%E2%80%94Tubular%20Rab10.mp4?dl=0
Supplementary Video 3: Neuron in mass culture expressing Rab10-EGFP (with intensity colour-coded as in Figure 4a) at steady state. The video is focused on an area of the cell body at the base of a primary neurite and show several Rab10-positive tubular structures moving in different directions are labelled with orange arrowheads. Dimensions and speed are indicated.